On the Design and Evaluation of Self-adaptive Network Architectures and Routing Protocols for Mobility Support

January 2012

Gen MOTOYOSHI

On the Design and Evaluation of Self-adaptive Network Architectures and Routing Protocols for Mobility Support

Submitted to
Graduate School of Information Science and Technology
Osaka University

January 2012

Gen MOTOYOSHI

List of Publications

Journal Papers

1. G. Motoyoshi, K. Leibnitz, and M. Murata, "Proposal and Evaluation of a Function-Distributed Mobility Architecture for the Future Internet," IEICE Transactions on Communications, vol. E94-B, no. 7, pp.1952–1962, July 2011.

2. G. Motoyoshi, K. Leibnitz, and M. Murata, "Evaluation and extension of Mobility Tolerant Firework Routing (MTFR)," conditionally accepted and under second review for IEICE Transactions on Communications, Special Section on Frontiers of Information Network Science, November 2011.

3. G. Motoyoshi, K. Leibnitz, and M. Murata, "Proposal and Evaluation of a Future Mobile Network Management Mechanism with Attractor Selection," submitted to EURASIP Journal on Wireless Communications and Networking, Special Issue on Recent Advances in Optimization Techniques in Wireless Communication Networks, January 2012.

Refereed Conference Paper

1. G. Motoyoshi, K. Leibnitz, and M. Murata, "Function-Distributed Mobility System for the Future Internet," in *Proceedings of the 5th IFIP/IEEE International Workshop on Broadband Convergence Networks (BCN 2010)*, April 2010.

2. G. Motoyoshi, K. Leibnitz, and M. Murata, "MTFR: Mobility Tolerant Firework Routing," in *Proceedings of the 4th International Workshop on Dependable Network Computing and Mobile Systems (DNCMS 2011)*, October 2011.

3. G. Motoyoshi, N. Wakamiya, and M. Murata, "Future Mobile Network Management With Attractor Selection," to be presented at *the 9th International Conference on Wireless On-demand Network Systems and Services (WONS 2012)* held in Courmayeur, Italy, January 2012.

Preface

Recently, there have been rapid changes in societies worldwide, such as explosion of the population, rapid growth of many developing countries, fatal blows by natural disasters and so forth. From the number of subscribers and the population, the penetration rate of mobile telephone in Japan is reaching 100 % and more than 100 million people enjoy mobile access to the Internet [1, 2]. These societal drastic transitions cause to change our sense of values and requirements for communication infrastructure from the user's perspective. As a result, communication infrastructures pay more attention to mission-critical systems, robustness to failures, and ease of use anywhere and anytime. In addition, more opportunities for people to use communication network services are produced and therefore more applications and traffic volumes are also generated. Hence, societal requirements have become so complicated that the current communication network researchers are struggling to meet them completely and they are now facing many challenging issues. High capacity, huge numbers of devices, high reliability, mobility as well as ecological and sustainable society support are among these challenging issues. We can see high activities in future Internet research efforts [3] in order to support the requirements above and make our future life more prosperous. Through the above discussion, we define mobility support, robust network management mechanism, and effective wireless technology usage as some of the most important issues for the future network.

Activities on solving these problems have started in the early 21st century and are gradually shifting from the research phase to the industrial phase depending on their arrangement which type of functions are equipped at which part of the communication network. From

the viewpoint of user needs for the future society, mobility support and wireless communication environment are essential anytime and anywhere, and as research activities for wireless future network research, there have been the MobilityFirst Project [4] of the FIA program and POMI (Programmable Open Mobile Internet) 2020 of the Stanford Clean Slate Program. They are both still in research phase. The investigation of the whole architecture and important protocols in detail are still desired. In order to cope with the above issue, we first design in this work a new architecture to divide mobility functions into several fractions and let each function be located in their appropriate position from the cost minimum viewpoint. Our proposed distributed mobility management method is qualitatively analyzed and quantitatively evaluated by computer simulation from the viewpoint of management cost, compared with conventional methods. The analysis and evaluation results show that our proposed method produces at high SMR (Signal-to-Mobility Ratio) about half of the cost of Mobile IP (MIP) extensions and roughly the same cost of MIP. On the other hand, at low SMR it has about the same cost as MIP extensions and 70% of the cost of MIP. Hence, it is confirmed that our proposed method has high flexibility to cope with overall conditions in all SMR ranges.

Second, from the viewpoint of robust network management mechanism, infrastructure-free systems of *Mobile Ad hoc Networks* (MANET) are very flexible in unstable network connectivity situations, for example after natural disasters, and they can cope with highly dynamic network topology changes due to node mobility. Potential based routing is one of the promising technologies to accomplish MANET-like routing in an autonomous manner. In order to avoid single points of failure, autonomous operation is one of the key factors. There have been several proposals for carrying out potential routing and the autonomous exchange of potential information among nearby nodes is the common basic approach for most of these protocols. Therefore, the time until convergence of potential updates and assurance of node reachability are suitable indicators for the performance of these routing protocols. Both reduction of convergence time and increase of packet reachability should be achieved at the same time in the future. In order to solve the above issue, we extend a potential based routing mechanism and we design a new routing protocol by adding a

broadcast function to adjust the place and area size for information flooding. Our proposed extended potential based routing is evaluated by computer simulation in terms of packet reachability and traffic overhead, compared with a conventional method. Simulation results show that we can observe an improvement of 20% in reachability at an additional cost of less than 3.5 hops transmission delay and less than two times traffic overhead as standard potential routing. As a consequence, our method has benefits of packet reachability performance at the cost of slightly additional traffic overhead and is sufficiently feasible for mobile system infrastructure.

Wireless access technologies have been rapidly developing these days, such as HSPA (High Speed Packet Access) on 3G cellular networks, WiMAX (Worldwide Interoperability for Microwave Access), LTE (Long Term Evolution), and WiFi (Wireless Fidelity). This kind of increase in diversity of access technology produces more convenience for our life and more complexity for management at the same time. Therefore, radio interface switching at the right time and at the right place is one of the key issues. However, mere progress in access technology is not enough and extended core networks to be in-line with this access technology are also necessary. From the core network viewpoint, there are several architectures suitable for the future mobile network with separated identifier and locator [5]. One of the most promising among these future Internet research activities is OpenFlow technology [6] to construct a programmable and environmentally-friendly ICET (Information, Communication, and Energy Technology) infrastructure [7–9]. The OpenFlow technology has a potential to meet a wide variety of requirements from users due to its programmability, which is available not only for wireless communication but also for wired. However, the above research projects are limited within local sites such as campus networks and data center networks for the time being. Hence, wider investigation is needed. In order to contribute to a solution of the above issue, we apply the attractor selection mechanism, which is a biologically inspired noise driven adaptation mechanism, to the multi-radio interface selection problem. We evaluate this biologically inspired mechanism to cope with multi-interface selection issue by computer simulation in terms of adaptability against changes of environmental conditions. It is confirmed by simulation that our proposed method can

work to adaptively select the best radio interface though wide range of SNR from 10 dB to 40 dB. As a result, we observe a reliable evidence for our method to work well.

As stated above, in this thesis, we design and evaluate self-adaptive network architectures and routing protocols for mobility support, which consist of the whole architecture with a novel distributed function placement, more reliable potential-based routing, and multi radio interface selection mechanism in an autonomous manner.

Acknowledgments

First and foremost, I would like to express my sincere gratitude to my supervisor, Professor Masayuki Murata of Graduate School of Information Science and Technology, Osaka University, for his providing me with an opportunity to research studies in this thesis with many researchers of ability under his directions. His patient encouragement, deeply insightful advice, creative suggestions, and precise guidance have been indispensable for my research activity.

I am heartily grateful to the members of my thesis committee, Professor Koso Murakami, Professor Makoto Imase, and Professor Teruo Higashino of Graduate School of Information Science and Technology, Osaka University, and Professor Hirotaka Nakano of Cyber Media Center, Osaka University, for reviewing my dissertation and providing many valuable comments.

I especially would like to express my appreciation to Invited Associate Professor Kenji Leibnitz of Graduate School of Information Science and Technology, Osaka University and also National Institute of Information and Communications Technology (NICT) for his continuously generous support and encouragement. This work would not have been possible without his patient encouragement, precise advice, and elaborated direction.

I am most grateful to Professor Naoki Wakamiya, Associate Professor Go Hasegawa, Associate Professor Shin'ichi Arakawa, Assistant Professor Yuki Koizumi, and Assistant Professor Shinsuke Kajioka of Osaka University, who provided me with helpful comments and feedback. Their instructively and scientifically critical comments and suggestions have been always informative and useful.

I am thankful to all the members of Advanced Network Architecture Laboratory in Graduate School of Information Science and Technology, Osaka University, for their inciting discussions and fellowship. We have formed a link through their friendliness characteristic of this laboratory and their kindness helped me a lot with my surviving the severe research life.

I would also like to thank to Executive Chief Engineer Toshiyuki Kanou, Central Research Laboratories of NEC Corporation, and General Manager Motoo Nishihara, Senior Engineer Yoshiaki Kiriha, Senior Expert Hirohisa Shiojiri, and Senior Manager Atsuhiro Tanaka, System Platforms Research Laboratories of NEC Corporation for giving me generous admission and constant support for my pursuit of the doctoral degree.

Finally, I want to thank my parents for their invaluable support and continuous encouragement in my life. I hope they are glad to see this thesis as a proof of my growth.

Contents

List of Figures

List of Tables

Chapter 1

Introduction

1.1 Background

Recently, there have been rapid changes in societies worldwide, such as explosion of the population, rapid growth of many developing countries, fatal blows by natural disasters and so forth. These societal drastic transitions cause to change our sense of values and requirements for communication infrastructure from user's perspective. As a result, communication infrastructures pay more attention to mission-critical systems, robustness to failures, and ease of use anywhere and anytime. In addition, more opportunities for people to use communication network services are produced and therefore more applications and traffic volumes are also generated. Hence, societal requirements have become so complicated that the current communication network researchers are struggling to meet them completely and they are now facing many challenging issues. High capacity, huge numbers of devices, high reliability, mobility as well as ecological and sustainable society support are among these challenging issues. We can see high activities in future Internet research efforts [3] in order to support the requirements above and make our future life more prosperous. Through the above discussion, we define mobility support, robust network management mechanism, and effective wireless technology usage as some of the most important issues for the future network.

In the current IP network era, *Mobile IP* (MIP) is the de facto standard mobility-supporting protocol [10, 11]. After Mobile IP was launched, several similar mobility protocols have been proposed, which are more efficient for handling specific objectives. Among them, *Fast MIP* (FMIP) [12] is suitable for carrying out fast handovers by using context transfer technology. On the other hand, *Hierarchical MIP* (HMIP) [13] has benefits in signaling cost reduction by using a localized binding update procedure with hierarchical network configuration. Furthermore, *Proxy MIP* (PMIP) [14] is well suited for *Mobile Node* (MN) workload reduction by shifting mobility functions up to the edge node. In addition, a hierarchical network configuration and centralized management system are commonly used in the mobility management of cellular networks. In next generation mobile networks, such as System Architecture Evolution/Evolved Packet Core (SAE/EPC) and Long Term Evolution (LTE), both GPRS-based (General Packet Radio System) and IP-based mobility management systems are considered and standardized [15, 16] for an all-IP mobile network and PMIP is adopted as IP-based mobility protocol. Gradually, IP mobility and cellular mobility are being harmonized and unified for future mobile networks. In the first part of this work, we propose a novel function distributed architecture to achieve the reduction of signaling cost in total.

As one of robust communication systems, infrastructure-free systems of *Mobile Ad hoc Networks* (MANET) are very flexible in unstable network connectivity situations, for example after natural disasters, and can cope with highly dynamic network topology changes due to node mobility. Potential based routing is one of the promising technologies to accomplish MANET-like routing in an autonomous manner. There have been several proposals for carrying out potential routing and autonomously exchanging potential information among nearby nodes is the common basic approach for most of these protocols. Therefore, the time until convergence of potential updates and assurance of node reachability are suitable indicators for the performance of these routing protocols. In addition, each potential routing scheme has its own benefits. However, as far as we know, few of them can deal with situations of highly changing topology caused by geographic movement of nodes. Therefore, we focus in the second part of this work on mobility oriented extensions of potential routing

in order to improve the data transmission reachability. In our approach, a data replication scheme like broadcast transmission is introduced to improve reachability. In addition, in order to avoid unnecessary broadcast traffic, a potential value is utilized as a measure for selection of broadcasters. The potential value of a node is an indicator of how close it is to the destination and therefore well suited for next-hop node selection.

From the viewpoint of user needs for the future society, a wireless communication environment is essential, and as research activities for wireless future network research, there have been several research activities such as the MobilityFirst Project [4] of the FIA program and POMI (Programmable Open Mobile Internet) 2020 of Stanford Clean Slate Program. In addition, there are several architectures suitable for the future mobile network with separated identifier and locator [5]. Among these activities, one of the most promising future Internet research activities is OpenFlow technology [6] to construct a programmable and environmentally-friendly ICET infrastructure [7–9]. The OpenFlow technology has a potential to meet a wider variety of requirements from users due to its programmability, which is available not only for wireless communication but also for wired. However, the above researches are limited within local sites such as campus networks and data center networks for the time being. In addition, from another point of view, robustness is one of the keywords when talking about the future Internet infrastructure for coping with disasters like huge Tsunami or earthquakes. In addition, energy saving corresponding to protection of the environment is also an important factor. To achieve the above targets, more reliable infrastructures based on theoretical background are desired instead of approaches based on empirical background. For instance, biological systems have evolved over a long period of time into systems of individuals where the essential factor is survival of the species and which are robust against environmental changes. That is the reason why such mechanisms have been frequently applied to the future ICET infrastructure. Speaking of biologically inspired control mechanisms, attractor selection is one example of the dynamics and bio-informatics theory to formulate a mathematical model. Recently, based on the above results, there have been many research activities with the attractor selection method adapted to the field of ICET management in the Yuragi Project [17] and in the Global Center of Excellence

Program for Founding Ambient Information Society Infrastructure [18]. In the third part of this work, we apply the attractor selection mechanism to solve radio interface selection issue, which alleviates elaborated tasks such as parameter adjustment and achieve cost reduction.

In order to establish the future mobile network possible to work in a wider scale and to achieve more flexible management for meeting the user's wider variety of satisfaction, the above-mentioned three issues, such as a flexible overall architecture, fluctuation tolerant routing protocol, and a lightweight management mechanism in a self-adaptive manner, become inevitable constituent components. Combined effects of these three factors provide us with satisfactory system establishment. In this thesis, we propose an architecture, a routing protocol, and a self-adaptive mechanism to cope with the above mentioned issues.

1.2 Outline of Thesis

In order to offer a solution which can cope with the above mentioned issues. We first study a novel mobility supported architecture, in this thesis. Then we propose a robust routing protocol based on gradient-based routing. Finally we investigate a self-adaptive mechanism to select the most appropriate candidates among two or more radio interfaces in one mobile node and dynamically construct the most cost-efficient clustering to avoid unnecessary inter-domain handovers.

A Function-Distributed Mobility Architecture for the Future Internet [19, 20]

In Chapter 2, we propose a function-distributed mobility management system [19] to provide a more efficient scheme leading to a more flexible system construction. We believe that this framework suits well to the requirements of the future Internet. We study the efficiency of our proposed method via a cost analysis based on location update cost and packet delivery cost and verify the validity of the cost analysis by computer simulation. Evaluation results

are shown comparing conventional mobility systems to our proposed one by performing a cost analysis with a random walk mobility model. Moreover, simulation results are shown and the validity of the analyses is confirmed.

MTFR: Mobility Tolerant Firework Routing [21, 22]

In Chapter 3, we propose an extended potential-based routing named Mobility Tolerant Firework Routing (MTFR). We first explain our proposed firework routing mechanism and then investigate and reveal basic tendencies and advantages of our approach from the viewpoint of efficient wireless communication. In addition, we especially pay attention to the relationship between transmission reachability and wireless coverage. The performance of our proposal is compared with conventional potential routing for the random walk and random waypoint mobility models. Before concluding this chapter, our proposed mechanism is analyzed from a theoretical viewpoint. Finally, we study an extension with a self-organizing mechanism and evaluate it by computer simulations.

Future Mobile Network Management With Attractor Selection [23, 24]

In Chapter 4, we investigate the combination of future mobile networks and attractor selection and we extend the basic attractor selection mechanism in order to work on large-scaled mobile wireless network environment based on OpenFlow technology. First, we discuss the future mobile network on a basis of combination of OpenFlow technology and the attractor selection method. Second, we propose a method for a mobile node to select the best radio interfaces according to environmental conditions with attractor selection using an activity driven by realtime user traffic volume. Finally, we establish an appropriate clustering method to reduce handover signaling cost on the OpenFlow based future mobile network with attractor selection using an activity driven by the difference of the flow directions between user traffic and signaling traffic. Simulation results show that the attractor selection

mechanism is feasible enough to work on a future mobile network.

Chapter 2

A Function-Distributed Mobility Architecture for the Future Internet

Several task forces have been working on how to design the future Internet in a clean slate manner and mobility management is one of the key issues to be considered. However, mobility management in the future Internet is still being designed in an "all-in-one" way where all management functions are tightly kept at a single location and this results in cost inefficiency that can be an obstruction to constructing flexible systems. In this chapter, we propose a new function-distributed mobility management architecture that can enable more flexible future Internet construction. Furthermore, we show the effectiveness of our proposed system via a cost analysis and computer simulation with a random walk mobility model.

2.1 Introduction

Recently, societal requirements have become so complicated that the current Internet is struggling to meet them completely and it is now facing many challenging issues. In order

to accomplish not only an incremental, but drastic innovation, many research works for new generation networks, in other words the future Internet, are being attempted from scratch all over the world. High capacity, huge numbers of devices, high reliability, as well as ecological and sustainable society support are among these challenging issues. We can see high activities in future Internet research efforts [3] in order to support the requirements above and make our future life more prosperous and it is easy to imagine that supporting user mobility is one of those critical functions.

Nowadays, several research task forces, such as AKARI [25] in Japan, have been working on future Internet research. Due to their efforts, we can see some classification of primary functions for the future Internet, such as security, content delivery mechanisms, delay tolerant networking (DTN), management and control framework, service architecture, routing, and future Internet infrastructure design for experimentation. As for mobility, it is one of the important features within the management/control framework and routing, and MILSA [5] seems to be one of the promising architectures dealing with mobility issues, such as multi-homing and ID/locator separation.

In the case of a mobility management system using geographically static anchors, supporting user mobility has some drawbacks in terms of the signaling cost and data transfer cost. Therefore, dynamically controlled mobility management systems are examined under various aspects. Wong et al. [26] show that a dynamic scheme outperforms a static scheme by assigning each user an own local area according to his profile. In addition, Ho et al. [27] and Li et al. [28] study a dynamic location update scheme from the viewpoint of location update cost and paging cost analysis. Chen et al. [29] propose a system to use dynamic location area management with minimum total cost. Choi et al. [30] distinguish MNs into several categories, such as predictable and unpredictable, and change the user's profile adaptively according to his mobility pattern.

In general, a centralized and static mobility management system is in the cases above regarded as the basic concept. However, such a management node could be a single point of failure and an obstruction to constructing a flexible system. Therefore, distributed systems have been studied under various aspects. Zheng et al. [31] propose a temporary home agent

in the visited network and perform dynamic Home Agent (HA) assignment in order to avoid a single point of failure and gain signaling cost efficiency at the same time. Yen et al. [32] use the anycast protocol to find the nearest HA and register there, which leads to cost reduction. Song et al. [33] propose another dynamic mobility management system with a flexible foreign agent grouping scheme and Bertin et al. [34] define a dynamic mobility to work in a flat network architecture in a distributed manner. Pack et al. [35, 36] and Singh [37] perform a cost analysis of HMIP compared with MIP and prove the effectiveness of HMIP.

In addition, from the viewpoint of mobility, IMS (IP Multimedia Subsystems) can offer session mobility handled by SIP (Session Initiation Protocol). This session mobility is maintained on IMS as service continuity. On the contrary, Mobile IP (MIP) and its extensions offer connection continuity on the network layer. Therefore, mobility management systems like MIP can coexist with session mobility systems like IMS, as can be seen in the current 3G mobile systems.

Several effective mobility methods have been examined up to date, however, all of them only consider a single mobility core function converged at a single node even though its geographical position can be dynamically changed. In other words, the mobility management function consists of several features such as *location management*, *authentication management*, *state management*, and so forth. Each of these sub-functions has its own characteristics and its own appropriate place to be located according to its characteristics. Therefore, a single mobility core function cannot accomplish to manage all these objectives at the same time and this leads to inefficiency in system management.

In this chapter, we propose a function-distributed mobility management system [19] to provide a more efficient scheme leading to a more flexible system construction. We believe that this framework suits well to the requirements of the future Internet. We study the efficiency of our proposed method via a cost analysis based on location update cost and packet delivery cost and verify the validity of the cost analysis by computer simulation. The rest of this chapter is organized as follows. In Section 2.2, we describe the design principles. Then in Section 2.3 the proposed function-distributed mobility system

is explained in detail. In Section 2.4, evaluation results are shown comparing conventional mobility systems to our proposed one by performing a cost analysis with a random walk mobility model. Moreover, simulation results are shown and the validity of the analyses is confirmed. Finally, Section 2.5 concludes this chapter.

2.2 Design Principles

In this section, the analytical mobility model and system parameters are discussed. Figure 2.1 illustrates the mobility model network configuration and an asterisk '*' indicates a delegated node in this figure. A *Mobile Node* (MN) is connected over a wireless link to a *Base Station* (BS) in a visiting network. All traffic between the MN and the remote destination is being relayed via *gateway* (GW) nodes to the *Home Agent* (HA) located in the home network of the MN. The values D_h, D_v, and D_c are the number of hops between each network and HA* represents the delegated node with a distributed mobility function. Figure 2.1 indicates the situation where the master HA in the home network executes the delegation of a function to a node labeled as HA* in the visiting network.

As in many other papers, we assume a hexagonal cellular mobility network model [36,37], where a *Mobility Anchor Point* (MAP) domain consists of the same number of rings and each ring r has $6r$ cells. Then, the number $N(R)$ of cells up to ring R is calculated as:

$$N(R) = \sum_{r=1}^{R} 6r + 1 = 3R\,(R+1) + 1.$$

In this chapter, we perform cost analysis by applying a random walk mobility model, which is a typical mobility model. The following subsection will show how the steady-state probabilities for a MN being in a certain cell r are obtained.

2.2.1 System Modeling

Figure 2.2 illustrates the one-dimensional Markov chain model that we use in this analysis. The number of each state corresponds to the ring number in the hexagonal cellular model.

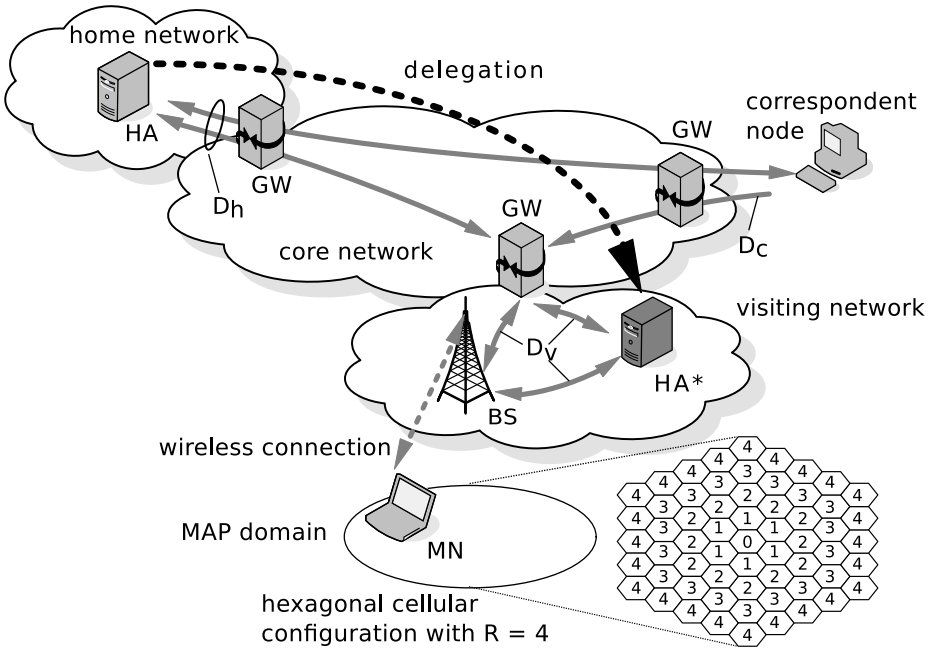

Figure 2.1: Mobility model network configuration

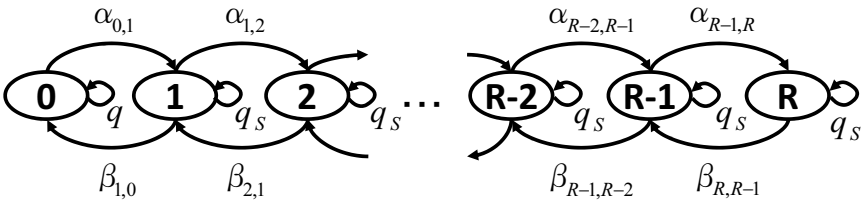

Figure 2.2: State diagram for random walk mobility model

We define q as the probability of the MN staying in the current cell and thus it moves to another cell with probability $1 - q$. In our model, an MN can either stay in its current concentric ring r or move to its outer $(r + 1)$ or inner $(r - 1)$ ring with equal probability. Therefore, the MN moves to other cells in ring r with the probability $q_S = (1 - q)/3$. In addition, it can move in an outward direction with the probability $p^+(r)$ and inward with $p^-(r)$.

$$p^+(r) = \frac{1}{3} + \frac{1}{6r} \qquad \text{and} \qquad p^-(r) = \frac{1}{3} - \frac{1}{6r} \tag{2.1}$$

Using the probabilities in Equation (2.1), we obtain the transition probabilities $\alpha_{r,r+1}$ and $\beta_{r,r-1}$ for an MN in an arbitrary ring r as in Equations (2.2) and (2.3).

$$\alpha_{r,r+1} = \begin{cases} 1-q & \text{if } r = 0 \\ (1-q)\,p^{+}(r) & \text{if } 1 \le r < R \end{cases} \tag{2.2}$$

$$\beta_{r,r-1} = (1-q)\,p^{-}(r) \qquad \text{if } 1 \le r \le R \tag{2.3}$$

Here, if we define $\pi_{r,R}$ as steady-state probability of state r within the MAP domain being composed of cells inside ring R, it is calculated as

$$\pi_{r,R} = \pi_{0,R} \prod_{i=0}^{r-1} \frac{\alpha_{i,i+1}}{\beta_{i+1,i}} \qquad \text{for} \quad 1 \le r \le R$$

$$\pi_{0,R} = \left(1 + \sum_{r=1}^{R} \prod_{i=0}^{r-1} \frac{\alpha_{i,i+1}}{\beta_{i+1,i}}\right)^{-1}$$

with $\sum_{r=0}^{R} \pi_{r,R} = 1$.

2.2.2 Cost Functions

In this section, the considered cost functions are defined. In order to conduct a fair evaluation of the true properties that each mobility management method has, the total cost for each method is analyzed without the paging cost. This is done because paging is not always supported by all methods, and existing studies like [28] indicate that paging cost is at most of the order of location update cost. Since all mobility methods use a similar paging-like function, the paging costs are nearly same irrespective of the mobility management method and we therefore expect that it does not have a large impact on the qualitative cost comparison. Therefore, the total cost

$$C_{tot} = C_{loc} + C_{pkt}$$

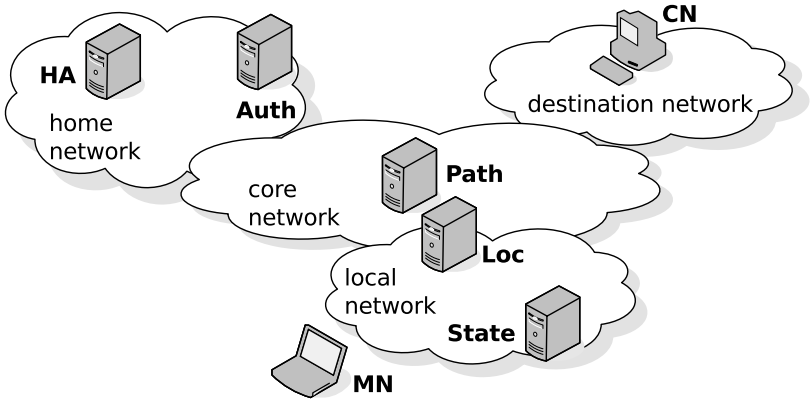

Figure 2.3: DisMob network configuration example

consists of the sum of location update cost C_{loc} and packet delivery cost C_{pkt}.

Location Update Cost Model

In HMIP, DynMob, and DisMob, there are location update procedures executed localized, whereas a global location update procedure is only done all the time in MIP. Here, *DynMob* is the abbreviation of *dynamic mobility* and indicates a single mobility core function that can be dynamically assigned via a temporary home agent [31], as shown in Figure 2.1. Also, *DisMob* stands for *distributed mobility* to indicate the system where the mobility function is divided into several sub-functions and each sub-function is dynamically assigned to different nodes according to their characteristics, see Figure 2.3. As stated above, we propose an architecture with finer granularity, such as a sub-function distribution scheme instead of an integrated management node, which makes it possible to construct more flexible systems. However, if an integrated system configuration is more suitable for the current situation of user distribution, traffic volume, and so forth, an integrated system configuration should be adopted.

Take the location update cost in DisMob for example. Let C_H, C_{LD}, and C_{LN} be the global location update cost, localized location update cost with delegation, and localized location update cost without delegation, respectively. Here, it is assumed that the most appropriate nodes for location and path management change as the MN moves within the

MAP domain and the delegation procedure for location and state management takes place even within a single MAP domain. Performing global location update means that the MN in the boundary ring R moves in an outward direction. In other situations, the MN performs a localized location update and in order to calculate the delegation probability, parameter ω is introduced as the probability with which the MN performs the delegation process. Here, the probability to perform global location update is calculated as $\pi_{R,R}\,\alpha_{R,R+1}$ and, therefore, the location update cost is calculated as follows:

$$C_{loc} = \frac{1}{\bar{T}}\left(\pi_R\,\alpha_{R,R+1} C_H + (1 - \pi_R \alpha_{R,R+1})\left[\omega\, C_{LD} + (1-\omega)\, C_{LN}\right]\right)$$

with

$$\begin{aligned} C_H &= 2\left[\kappa + \tau\left(D_v + D_h\right)\right] + N_{CN}\left(2\left[\kappa + \tau\left(D_v + D_c\right)\right] + PC_{CN}\right) \\ &\quad + PC_{HA} + PC_{HA_d} + PC_{HA_d^*} \end{aligned} \tag{2.4}$$

$$C_{LN} = 2\left(\kappa + \tau D_v\right) + PC_{HA^*} \tag{2.5}$$

$$\begin{aligned} C_{LD} &= 2\left(Z_s\, Y_s + Z_l Y_l\right)\left(\kappa + \tau D_v\right) + 2\, Z_p\, Y_p\, N_{CN}\left[\kappa + \tau\left(D_v + D_c\right)\right] \\ &\quad + PC_{HA^*} + PC_{HA_d^*} + PC_{HA_d^{**}} \end{aligned} \tag{2.6}$$

where $\bar{T}$ is the average cell residence time and κ and τ are the unit transmission costs for wired and wireless links, respectively. Here, $\bar{T}$ is calculated as the average time period for a mobile user to stay in the same cell, D_h, D_c, and D_v are the number of hops in each traversed network, and N_{CN} is the number of CNs (*Correspondent Nodes*) that the MN communicates with; PC_{xx} represents the processing costs for binding update procedures at each node, where '*' means that the costs are caused by the delegation process; '*' with and without 'd' means the costs to be delegated by another node and to delegate a sub-function to another node, respectively. In this chapter, PC_{HA^*} is assumed equivalent for PC_{HA}, PC_{HA_d}, and $PC_{HA_d^*}$, while $PC_{HA_d^{**}}$ is equivalent to $PC_{HA_{MAP}}$. Finally, $Y_{s/l/p}$ and $Z_{s/l/p}$ are delegation probability parameters for state, location, and path management, respectively. $Y_{s/l/p}$ indicates the cost reduction improvement ratio by delegation and delegation

starts only when cost reduction effects are expected to be obtained by delegation. $Z_{s/l/p}$ indicates the ratios of the cost by each function process to the overall cost. Therefore, the sum over $Z_{s/l/p}$ is 1. Although our system has four types of distributed functions, *authentication* is only performed initially and then at a low frequency, which is the reason why we will not include the authentication process in our cost analysis. In addition, in our model, transmission delay, as the number of hops in each traversed network, and cost for function delegation are taken into account which permit a fair evaluation by including merits and demerits of our proposed method.

Let us discuss C_H as expressed in Equation (2.4) as example. When the MN sends a location update message toward the HA in the home network, it will be first transferred over a wireless link to a BS in the visiting network, then over a wired links to a GW between visiting and core network in the visiting network, then to the GW between home and core network in the core network, until it finally reaches the HA via a wired link in the home network. The location update response message from the HA will retrace these steps to the MN. The costs C_{LD} and C_{LN} in Equations (2.5) and (2.6) are derived in the same way.

We should also remark that in the case of DisMob, there will be interactions among each sub-functions. For example, location management and path management will choose the best delegation node for an MN using its state information. If the MN accesses each sub-function management node securely, it also needs to use the authentication management function. In addition, each sub-function itself may be distributed on a user-by-user basis requiring each function to coordinate with each other. However, in this chapter, this kind of cost by interaction processes is assumed to be accommodated within the delegation cost. We plan to extend the cost analysis to interaction process cost in future work. The location update costs for MIP, HMIP, and DynMob are calculated in a similar way and the equations can be found in the appendix.

Packet Delivery Cost Model

In this section, packet delivery cost is calculated. First, $N_{MN} = N_{AR}\,K$ is the total number of users in the current MAP domain and it is the product of the number N_{AR} of *Access*

Routers (ARs) in the current MAP domain and the average number of users K within the coverage of an AR. Here, an AR is assumed to be located in a cell. Since N_{AR} is equivalent to the number of cells $N(R)$ in the MAP domain, the number of MNs N_{MN} increases with R.

Then, the packet delivery cost is expressed as follows, where C_{MAP}, C_{HA}, and C_T are processing costs for packet delivery at MAP and HA, and the packet transmission cost from CN to MN, respectively.

$$C_{pkt} = C_{MAP} + C_{HA} + C_T \tag{2.7}$$

Firstly, C_{MAP} is in general divided into two parts, such as lookup and routing cost. Lookup cost is proportional to the mapping table size, i.e., the number of MNs. On the other hand, routing cost is known to be proportional to the logarithm of the number of ARs in the MAP domain [35]. Secondly, in terms of C_{HA}, route optimization only lets the first packet transit the node which has the function corresponding to the HA. All following packets of the session are transferred directly to the MN. Thirdly, C_T is the transmission cost and it depends the distance, i.e., the number of hops between MN and CN. Finally, according to the discussion above, the total packet delivery cost is calculated as follows:

$$\begin{aligned} C_{pkt} = \lambda_s \big(& \bar{S} \left[w_{MN} N_{MN} + w_{AR} \log(N_{AR}) \right] + \theta_{HA} \\ & + \tau \left[(\bar{S} - 1)(D_c + D_h) + (D_h + D_v) \right] + \kappa \bar{S} \big) \end{aligned}$$

where λ_s, $\bar{S}$ and θ_{HA} are the session arrival rate, average session size in units of packets, and unit packet processing cost, respectively. The terms w_{MN} and w_{AR} are used as weighting factors.

2.3 System Description

In the current mobility management system, all mobility-related functions are "all-in-one" and centrally located in the same place. However, each function has very specific characteristics of its own that each function should be divided and located at its own appropriate

place in a dynamical manner. For that reason, we propose a function-distributed mobility system and this distribution mechanism is performed by a delegation procedure. The details of this scheme are explained in this section.

2.3.1 Function-Distributed Mobility Architecture

In this section, we explain the function-distributed mobility system. First, Figure 2.3 briefly sketches a network configuration example supporting function-distributed mobility (DisMob). In typical cases, the whole network consists of home network, core network, local network, destination network, and mobile node. Home network is where the mobile user is registered, destination network is where the targeted CN is connected, local network is where the MN is currently visiting, and core network connects all the above-mentioned networks. *Auth*, *Path*, *Loc*, and *State* in Figure 2.3 are all distributed and delegated function elements.

Next, a basic delegation sequence procedure is shown in Figure 2.4. The MN starts to send a registration request to a pre-defined *master node*, which is named as HA in Figure 2.4, after power on and the network attachment procedure, and then the MN and master node maintain the connecting path information. At the master node, fault recovery time is calculated with database information of the environment using real-time information if possible. After that, the master node selects the most appropriate node for each function to be delegated according to the information above and starts to execute the delegation procedures. After all delegations have been successfully completed, the master sends an acknowledgement signal to the MN. Finally, the MN can communicate with the CN and receives optimal function-placed service leading to optimal cost.

In addition, the layer structure is shown in Figure 2.5. On user plane, there is no difference from the conventional communication layer structure like the OSI model. As for the control plane, the function delegation procedure is of course required and flexible path management such as user-based management follows, which is a key factor of function-distributed mobility. In addition, each distributed function should be kept automatically

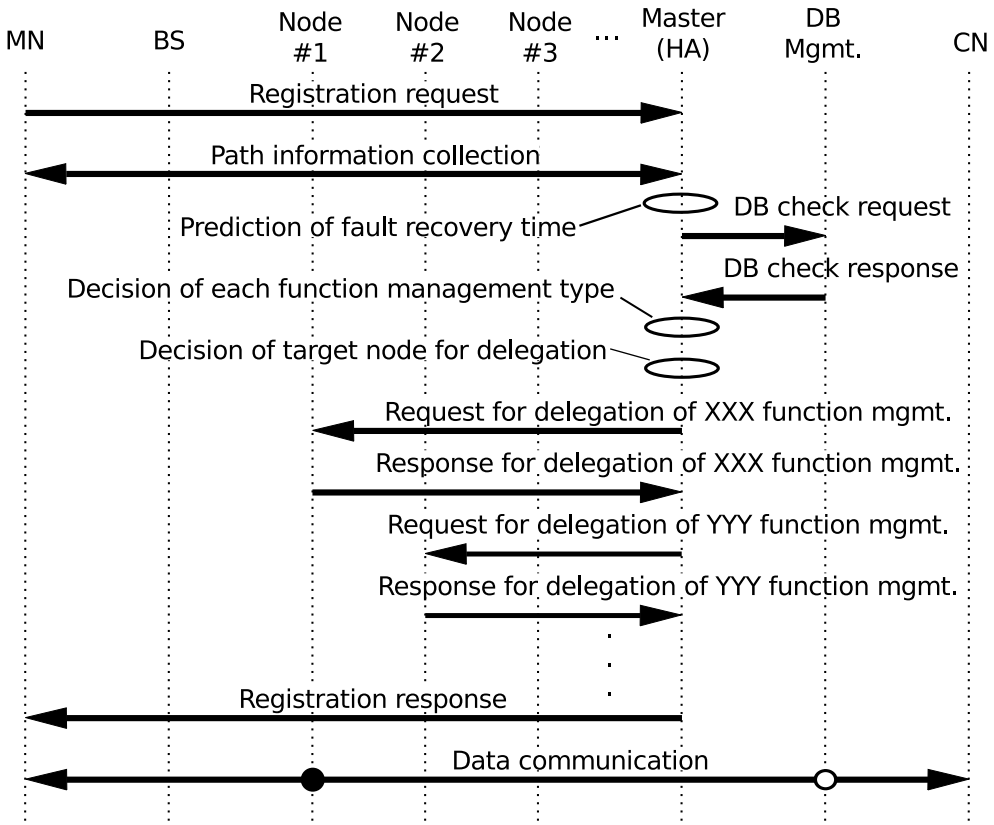

Figure 2.4: Basic sequence of delegation procedure

and dynamically updated. Finally, the management plane accommodates each distributed function management entity.

2.3.2 Features of Function-Distributed Mobility

As for the function-distributed mobility, the appropriate placement of each function is of great importance. Table 2.1 represents the impact of each function management scheme from mobility system parameters. Most mobility system parameters are dynamically updated and the higher the impact is, the closer the distributed function should be located to the MN. Therefore, the *authentication function* should be located deep inside the network, e.g., in the home network, while the *state function* should be located at the nearest node in the visited local network. In addition, the *path management function* should be located

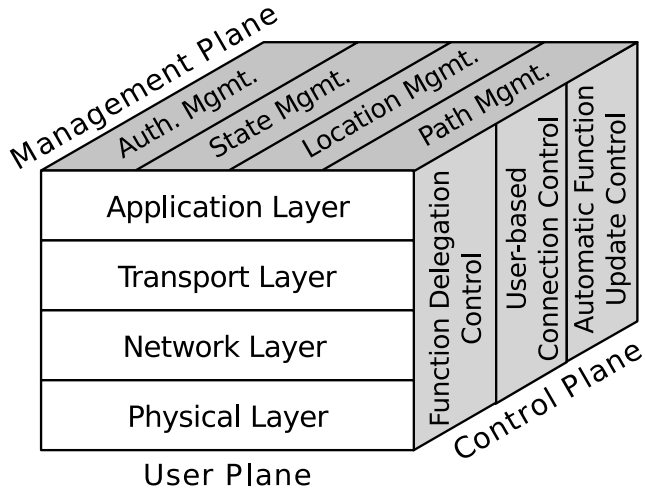

Figure 2.5: Layered structure of function-distributed mobility

somewhere in-between the source and destination, e.g., in the middle of the core network, to cope with fast switchover of paths. Finally, the *location management function* consisting of both anchoring and casting should be placed at intermediate locations, e.g., in the middle of the local network, where it is near to the core network and also the MN. Here, *anchoring* is the function that a specific node provides a constant presence of static IP address for the MN and works like an anchor to support loss-less communication to user movement. The *casting function* multicasts user data toward potential nodes that the MN moves in advance to support user movement.

This distribution does not lead to a mere tradeoff between efficiency and management cost. As stated earlier in Section 2.3.2, each location of sub-functions in Figure 2.3 illustrates one type of ideal conditions. This distributed disposition of sub-functions makes it possible for us to carry out well-shaped and well-optimized location update processes. For instance, mobile nodes and a mobile infrastructure only have to follow well-optimized location update processes, meaning that messages with minimum necessary payloads can be exchanged along minimum necessary routes on each occasion.

Table 2.1: Impact of each function placement from mobility system parameters (H:high, M:medium, L:low)

Parameter	Each mobility function				
	Anchor	*Cast*	*Path*	*State*	*Auth*
Access frequency	H	M	M	H	L
MN speed	M	H	H	H	L
Recovery time	M	H	H	H	L
Traffic volume	M	H	H	L	L
MN number	L	M	M	H	M
Application type	M	L	H	H	L

2.3.3 Comparison between Function-Distributed and Conventional Mobility Systems

In this section, function-distributed mobility is compared with MIP, HMIP, DynMob, and LTE in terms of mobility specific metrics, such as location update procedure type, anchor point flexibility, function distribution, and path management capability.

Table 2.2 indicates a qualitative comparison with other conventional mobility methods. From the viewpoint of location update type, MIP executes all the time a global registration whereas the other methods have the ability of using a localized and cost-efficient registration process. In terms of anchor point flexibility, MIP and HMIP basically use a fixed point. However, the other schemes could change their anchor point dynamically according to user preferences and environment conditions. As for function distribution, which leads to a flexible system construction, distributed mobility is the only way to accomplish this feature. Also only DisMob has the ability to manage transit paths from source to destination. These two functions are key differentiating factors between DisMob and conventional systems.

Table 2.2: Qualitative comparison between mobility systems

	MIP	HMIP	DynMob	LTE	DisMob
Location update	global	global, local	global, local	global, local	global, local
Anchor point	fixed	fixed	*dynamic*	*dynamic*	*dynamic*
Function "all-in-1"	yes	yes	yes	yes	*no*
Path management	fixed	fixed	fixed	fixed	*flexible*

Table 2.3: Basic system parameters used in the DisMob evaluation

PC_{CN}	PC_{HA}	PC_{HA^*}	PC_{HAd}	PC_{HAd^*}	$PC_{HAd^{**}}$
6	24	24	12	12	12
θ_{HA}	θ_{HA^*}	N_{AR}	N_{CN}	ω	γ
20	20	1	2	0.55	0.43
Z_s	Z_l	Z_p	Y_s	Y_l	Y_p
0.1	0.6	0.3	0.7	0.7	0.7
τ	κ	K	D_h	D_c	D_v
1	2	4	6	4	2
w_{MN}	w_{AR}	$\bar{S}$	q	λ_s	
0.1	0.2	10	0.4	0.1	

2.4 Numerical Evaluation

In this section, we show numerical results based on the mobility system we discussed in Section 2.3. First of all, the system parameters are shown in Table 2.3, which are following previous works that we believe are realistic [36]. All parameters are the same that appeared in previous sections, except for the delegation parameter for DynMob γ. Four methods, MIP, HMIP, DynMob, and our proposed DisMob are evaluated by their costs in the following section.

2.4.1 Simulation Settings

While our focus lies on the analytical evaluations, we also show results from computer simulation to validate our numerical analyses. Simulation conditions are shown in Table 2.4. In general, we assume the same conditions for the simulations and numerical analysis as much as possible. Mobile nodes are simulated to move in a random walk manner within hexagonal cellular fields and establish connections with the correspondent node according to the session arrival rate. In order to compare numerical analysis and simulation, an ideal wireless condition is assumed in simulations and our computer simulation program is implemented in the C programming language. Each plot shows the average of 100 simulation runs, corresponding to 100 different random seeds. We show numerical evaluation results for parameters given in Table 2.3 and for MAP domain sizes $R = 1$ and $R = 4$. We show the results for $R = 1$ since they can be regarded as baseline and $R = 4$ because they revealed the most interesting phenomena including crossover points of cost. Other values of R yielded similar results following a nearly linear tendency.

2.4.2 Location Update Cost Analysis

One of the most characteristic features in mobility systems is the location update procedure. Therefore, location update cost is evaluated first. Figures 2.6(a) and 2.6(b) show the location update cost against average cell residence time for MAP domain sizes $R = 1$

Table 2.4: Simulation conditions

parameter	**value**
simulation field	hexagonal cellular
mobile node movement	random walk
mobility speed	10 [m/s]
session arrival rate	0.1
traffic type	constant bit rate
wireless link	ideal (no packet loss)
simulation time	1,000,000 [s]

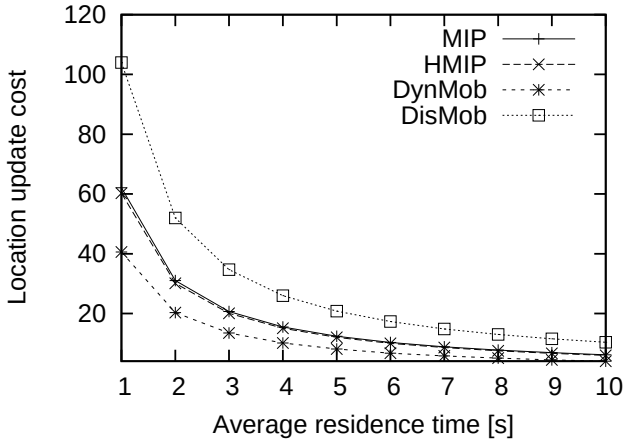

(a) $R = 1$

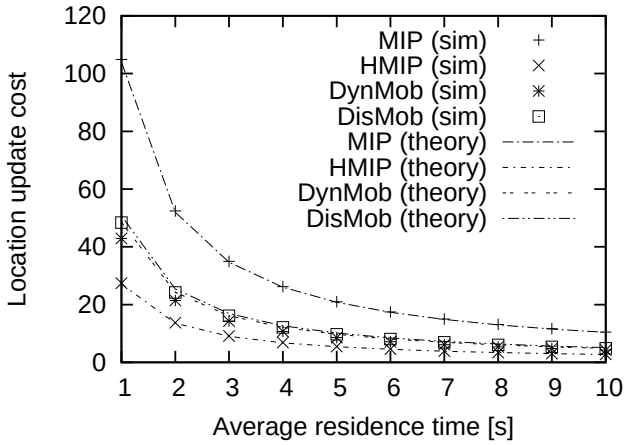

(b) $R = 4$

Figure 2.6: Location update cost over residence time

and $R = 4$, respectively. Location update costs are closely related to user mobility and cell residence time is regarded as a good indicator for that. Therefore, location update cost decreases as cell residence time increases. In addition, the smaller the MAP domain size R is, the more often an MN also performs a global location update rather than a localized location update. For comparison, location update cost normalized by the number of handovers normalized by simulation time are used as simulation results. It can be seen that the simulation results fit well with theoretical values.

HMIP, DynMob, and DisMob show better performance than MIP. This is because these three methods can perform a localized location update process to omit location update cost as long as the MN moves within a small localized area. On the other hand, MIP has to perform global location updates all the time. This property also explains the fact that the cost in HMIP, DynMob, and DisMob decreases as the MAP domain size R increases, whereas the costs in MIP is independent of R. Besides, we could see some small difference among the results by these three methods and they are simply caused by the delegation cost in the case of DynMob and DisMob. Unlike HMIP, DynMob requires a delegation process and DisMob needs a more precise delegation process than DynMob. Therefore, the delegation cost of DynMob is smaller than that of DisMob. As a result of this section, the methods other than MIP seem to be the better solutions just from the viewpoint of location update cost.

2.4.3 Packet Delivery Cost Analysis

Next, the packet delivery cost is evaluated in this section, which is another typical metric for mobility system evaluation. The packet delivery process is closely related to user population, whereas location update cost is influenced by user mobility. In other words, packet delivery cost increases with the number of MNs in the MAP domain. From most previous works [35, 36], it is well-known that the lookup procedure to confirm whether the targeted MN is registered in the mapping table or not is the most costly process. In our previous work, we analyzed packet delivery cost against number of MNs in a cell [19].

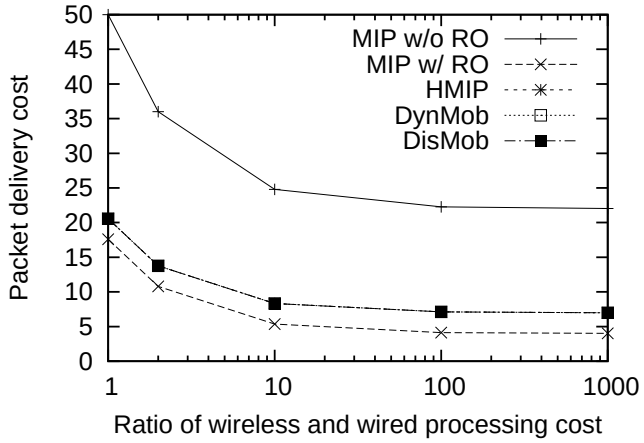

(a) $R = 1$

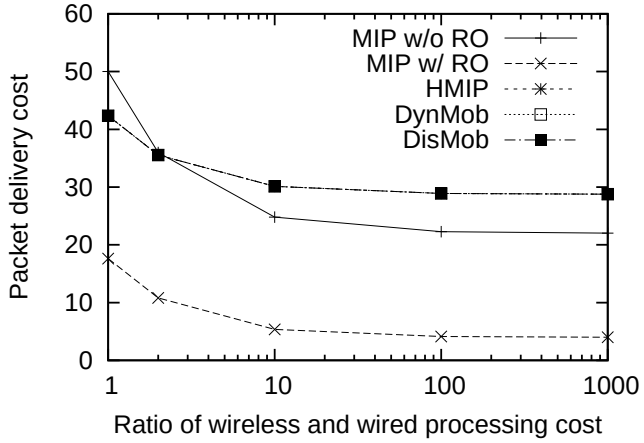

(b) $R = 4$

Figure 2.7: Packet delivery cost over wireless and wired processing cost ratio

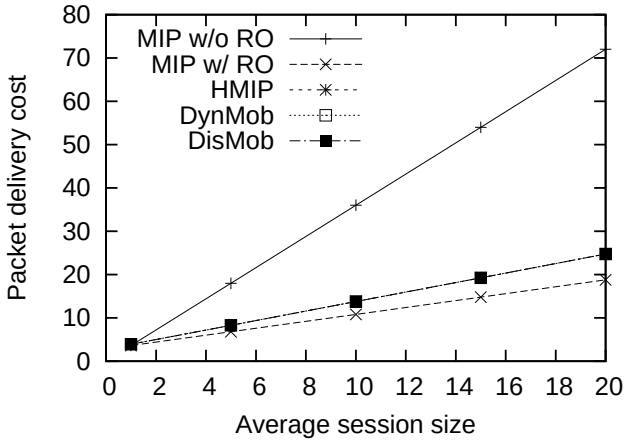

(a) $R = 1$

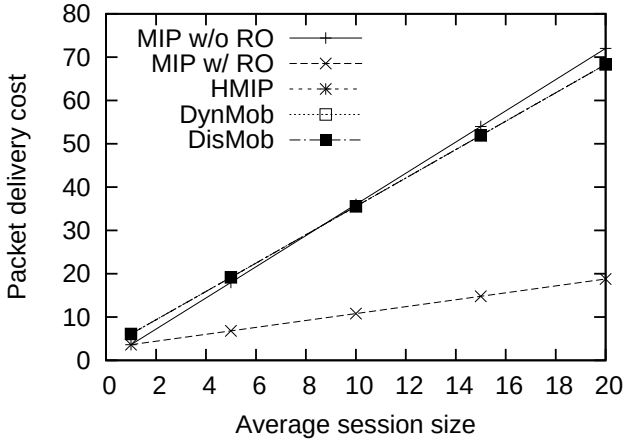

(b) $R = 4$

Figure 2.8: Packet delivery cost over session size

Furthermore, the wireless communication environment is rapidly growing these days. The growth of wireless processing cost is observed and the amount of data transmission over the wireless link is growing steadily. From this point of view, wireless and wired processing costs and average session size are important factors for evaluating mobility systems.

First, Figures 2.7(a) and 2.7(b) show the packet delivery cost against ratio of wireless and wired processing cost for MAP domain sizes $R = 1$ and $R = 4$, respectively. The wireless and wired processing costs are τ and κ, respectively, so by keeping a fixed wired processing cost of $\kappa = 2$, we can observe different ratios κ/τ. Just for reference, MIP results with and without route optimization (RO) are also given in this evaluation. The other three methods except for MIP show the same performance results and this is because packet delivery cost is heavily dependent on the route of packet delivery and session arrival rate. In MIP, packet delivery costs are same for $R = 1$ and $R = 4$, whereas in the other three methods it is higher for $R = 1$ than for $R = 4$. For smaller MAP domain size $R = 1$, costs in the other three methods are closer to that of MIP with RO. On the other hand, with larger MAP domain size $R = 4$, the costs in the other three methods approach those of MIP without RO and a crossover point at a ratio of about 2, which is well within the practical processing cost range, is seen. The other three methods show better results at lower ratio, while MIP without RO is better at higher ratio. The crossover point appears because the lookup procedure cost in the three methods except for MIP is linear to the number of MNs in a cell and MIP has constant behavior to perform the same transmission mechanism using the MIP tunnel.

Figures 2.8(a) and 2.8(b) show the packet delivery cost against average session size, with respect to transmission data volume such as a unit of bytes for $R = 1$ and $R = 4$, respectively. The other three methods except for MIP show identical values due to the same reasons stated earlier. It is obvious that the cost increases linearly with the average session size. Again, the costs for the other three methods are closer to that of MIP with RO when $R = 1$, whereas it is closer to that of MIP without RO when $R = 4$. A crossover point appears at *average session size* $= 10$.

From these results, MIP especially with RO seems to be the best solution, just from

the viewpoint of packet delivery cost. The management of system configuration and cost reduction are effective in making good use of these crossover point properties.

2.4.4 Total Cost Analysis vs. SMR

In the previous two sections, we could find benefits for each of MIP and the other three methods via location update and packet delivery cost analysis. In this section, the total cost is evaluated as the sum of both.

For evaluation of mobility systems, *Session-to-Mobility Ratio* (SMR) is commonly used as metric, which is a mobile packet network's counterpart of Call-to-Mobility Ratio in Personal Communication Service (PCS) networks. SMR is the relative ratio of the session arrival rate to user mobility. Here in the random walk model, SMR is defined as $\lambda_s \bar{T}$.

Figures 2.9(a) and 2.9(b) present the total cost analysis against SMR for $R = 1$ and $R = 4$, respectively. The three methods show almost the same performance as in location update and packet delivery cost analysis. MIP shows a cost beneficial behavior for higher SMR and the other methods for lower SMR. Around SMR = 1 is the borderline where the tendency is turned over and this phenomenon is clearer at large MAP domain size.

In addition, Figures 2.10 and 2.11 present the total cost against ratio of wireless processing and average session size, respectively. The three methods show almost the same performance as for the ratio of wireless processing and average session size. From Figure 2.10, MIP with RO shows cost beneficial behavior in most ratios, however, the other three methods have potential to improve to higher levels in the future when wireless exceeds wired communication conditions, which means lower ratio than 1. Also, from Figure 2.11, MIP with RO shows cost beneficial behavior in most average session sizes, however, in the case of $R = 4$, an average session size between 5 and 8 appears as turning point where the other three methods become the most cost beneficial.

As for total cost versus MAP domain size R, the increase of R has no impact on MIP in terms of total cost. However, especially at low SMR such as 0.1, the minimal total cost in the other three methods is reached for MAP domain size $R = 2 \sim 3$ and in case of high

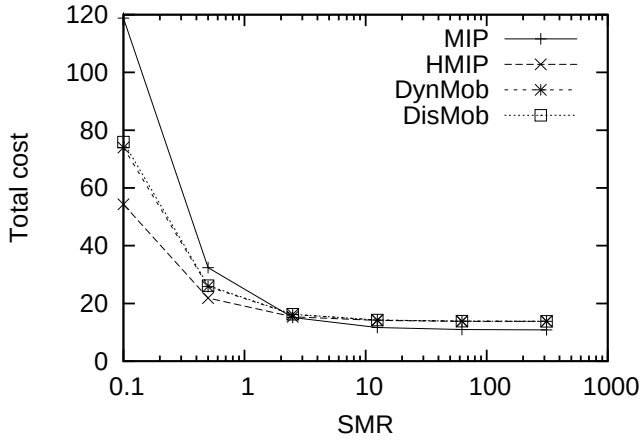

(a) $R = 1$

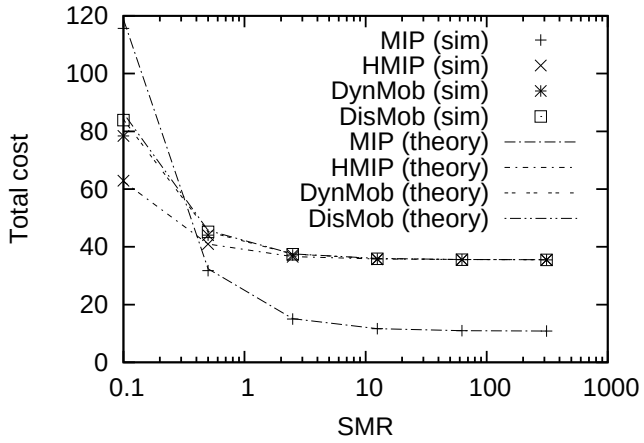

(b) $R = 4$

Figure 2.9: Total cost over SMR

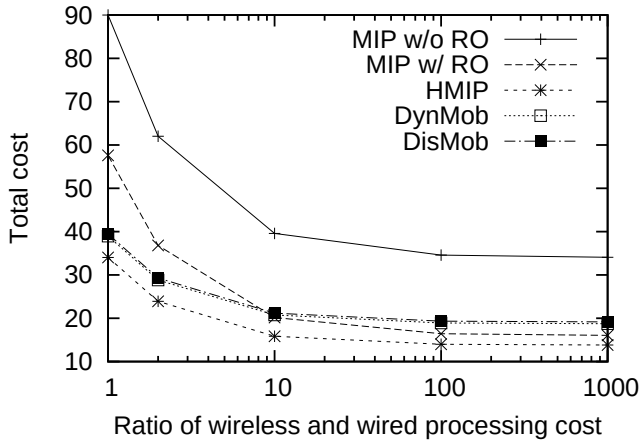

(a) $R = 1$

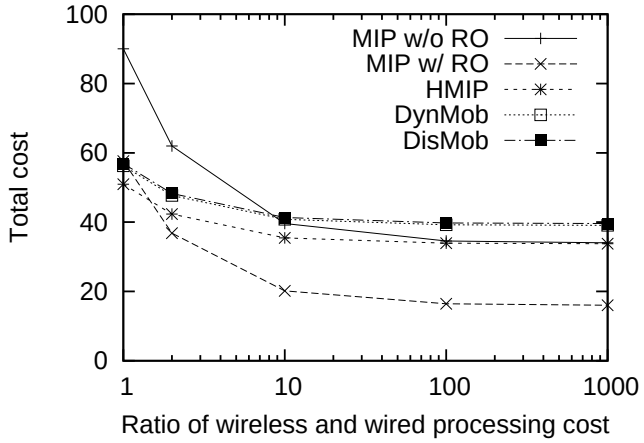

(b) $R = 4$

Figure 2.10: Total cost over wireless/wired processing cost ratio

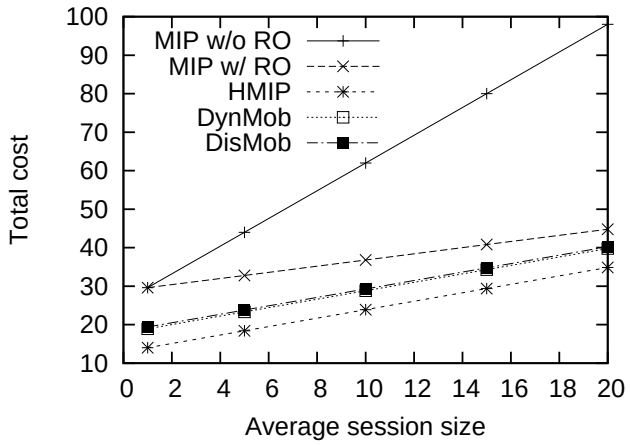

(a) $R = 1$

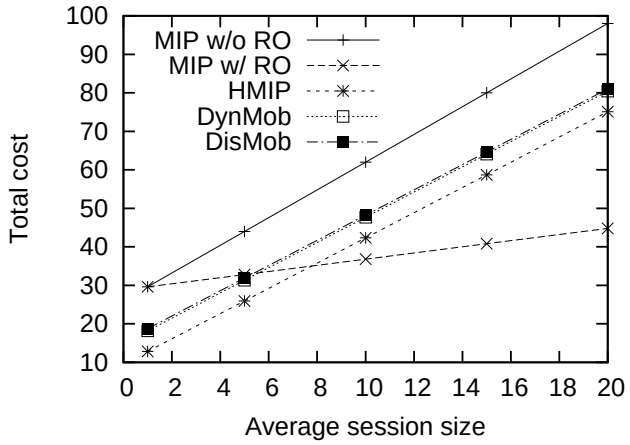

(b) $R = 4$

Figure 2.11: Total cost over session size

SMR, it increases almost linearly with R. This tendency towards an optimal MAP domain size is only visible for the total cost analysis and not for location update and packet delivery costs.

In summary, MIP with RO tends to be beneficial in most cases, however, the other three methods can become good candidates in some specific conditions.

2.4.5 Fair Evaluation by Total Cost Analysis

Until here, the benefits of the three methods except for MIP have been confirmed by cost analysis at equal MAP domain sizes. Delegation imposes additional costs compared to mobility management without delegation. Therefore, on comparison between different mobility methods at equal MAP domain sizes, the methods with delegation may appear worse from the cost view. However, if we compare costs under the condition of the same localized area size, where no delegation is necessary, the cost increase by delegation management and cost reduction by delegation efficiency effects can be investigated and evaluated. For this reason we consider this type of evaluation fairer than those in the previous sections.

Figure 2.12 presents the unified localized area concept. In case of DisMob, according to the probability ω, the delegation procedure is assumed to be executed, i.e., the area of no-delegation corresponds to the area expressed by $1-\omega$. Similarly, in case of DynMob, according to the probability γ, the delegation procedure is assumed to be executed, i.e., the area of no-delegation corresponds to the area expressed by $1-\gamma$. In order to equalize the localized area among all considered systems, i.e., the area without delegation, we adjust delegation parameters γ and ω. First, we select $R=3$ for HMIP, $R=2$ for DynMob, and $R=1$ for DisMob in order to have a margin for producing a potential overlap. Then, we calculate the localized area size for each method using γ and ω. Finally, each localized area size is unified by adjusting γ and ω as follows.

$$\frac{1-\gamma}{\gamma} = \frac{9\pi R^2}{16\pi R^2 - 9\pi R^2} \qquad \Rightarrow \qquad \gamma = \frac{7}{16}$$

$$\frac{1-\omega}{\omega} = \frac{4\pi R^2}{9\pi R^2 - 4\pi R^2} \qquad \Rightarrow \qquad \omega = \frac{5}{9}$$

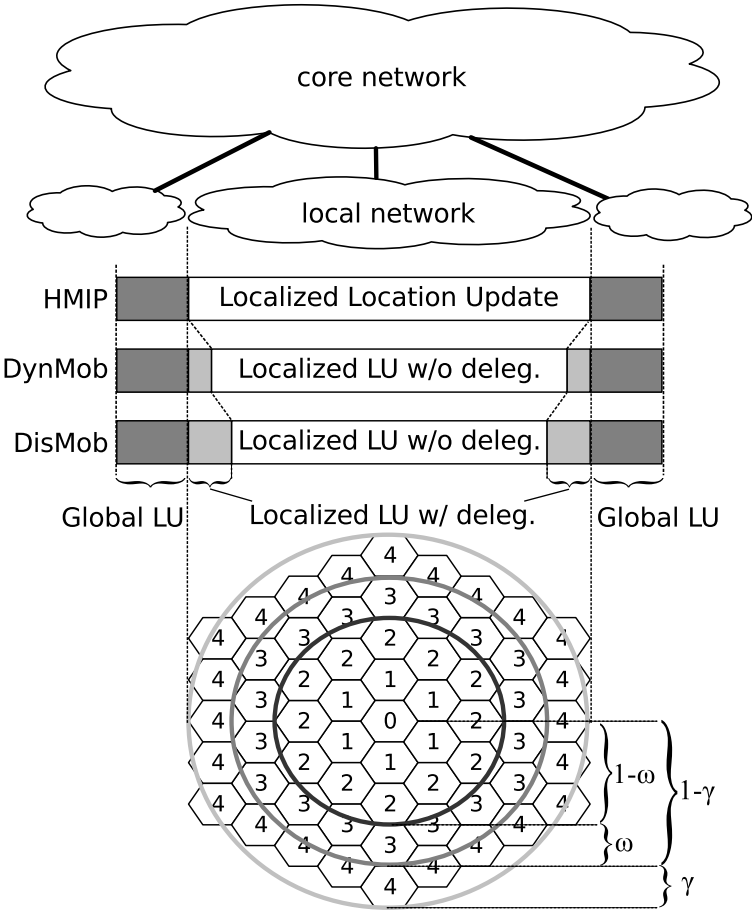

Figure 2.12: Concept of localized area

Figures 2.13 and 2.14 represent the cost for location update and packet delivery in a unified local area, respectively. From Figure 2.13, HMIP still shows the best performance among the three dynamic methods. However, from Figure 2.14, DisMob shows the best performance among the three when we consider packet delivery cost. This is because delegation cost itself seems to have a closer relationship with location update cost, but packet delivery cost has a closer relationship with MAP domain size.

Figure 2.15 shows the total cost analysis in the unified local area. In SMR above 10, MIP with RO shows the best performance followed by DisMob. In the medium range of SMR around 1, DisMob shows the best performance, and for SMR less than 1, HMIP shows the best performance followed by DynMob and DisMob. In summary of these results, MIP

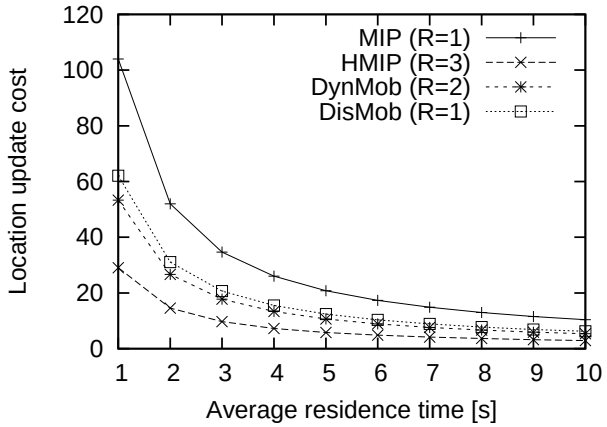

Figure 2.13: Location update cost analysis in unified local area

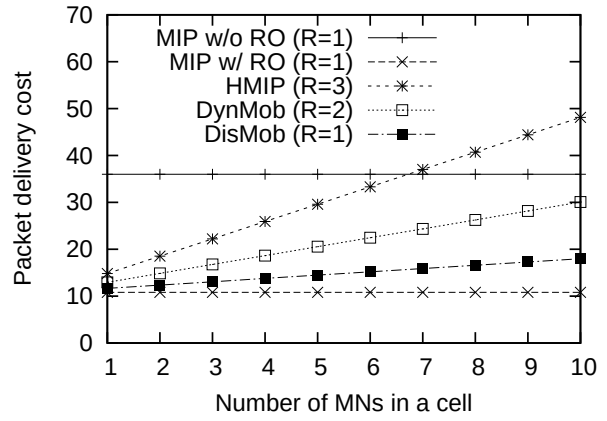

Figure 2.14: Packet delivery cost analysis in unified local area

has a slight advantage at higher SMR, but disadvantages at lower SMR, while HMIP has a slight advantage at lower SMR, but disadvantages at higher SMR. On the other hand, DisMob outperforms DynMob in most SMR ranges. As a consequence, DisMob has high flexibility to cope with overall conditions in all SMR ranges.

2.5 Conclusion

In this chapter, we proposed a function-distributed mobility architecture for the future Internet. First, we showed qualitative benefits of our proposed method. Then, compared

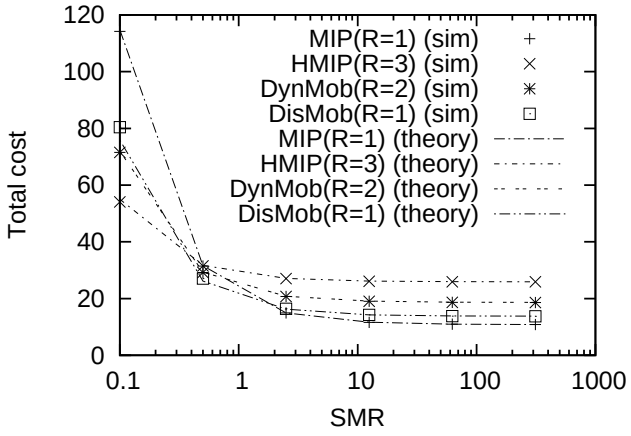

Figure 2.15: Total cost analysis in unified local area

with conventional MIP, HMIP, and DynMob, location update cost and packet delivery cost were analyzed for a random walk mobility model from the viewpoint of SMR. The cost analysis showed that HMIP, DynMob, and DisMob have a similar performance and a better performance than MIP. At higher SMR, MIP has more benefits, however at lower SMR, the other three methods are better. In addition, we showed that our proposed function-distributed mobility method showed better performance by cost analysis on a unified localized area in order to cope with overall SMR environment at the same time. Finally, we shared simulation results, confirmed the validity of our numerical analysis, and showed that our proposed function-distributed mobility method is effective and flexible.

In our future work, we are planning to include the effects of paging cost and interaction process cost, different mobility models, and more realistic parameter fluctuations, as well as further analytical studies and efficient function placement.

Chapter 3

MTFR: Mobility Tolerant Firework Routing

In this chapter, we propose a novel mobility assisted and adaptive broadcast routing mechanism called *Mobility Tolerant Firework Routing* (MTFR) that improves node reachability, especially in situations with high mobility. We evaluate our proposal by simulations with the random walk and random waypoint mobility models and disclose tendencies that can be observed with regard to typical parameters for wireless communication. As a result, our proposed method produces better reachability in many aspects at the expense of a small additional transmission delay and intermediate traffic overhead. Furthermore, some specific nonrecoverable conditions are revealed due to wireless coverage density. Theoretical analysis of connectivity for static node distributions and an extension with adaptive parameter management are also presented in this chapter. Our results show that MTFR is a promising routing protocol and feasible for future Internet infrastructures.

3.1 Introduction

Recently there has been increased research on future Internet infrastructures among researchers in the field of ICT (Information and Communication Technology) and new basic

principles of network management are currently being developed. From the viewpoint of the societal requirements toward a prosperous future, one goal of the future Internet is to pursue and guarantee reliability and efficiency at the same time. In addition, ubiquitous mobility and wireless communication is anticipated to play an even more essential role in the future. In other words, flexibility and simplicity of mobile network management will bring us a more comfortable life at the cost of an increased management complexity.

Infrastructure-free systems of *Mobile Ad hoc Networks* (MANET) are very flexible in unstable network connectivity situations, for example after natural disasters, and can cope with highly dynamic network topology changes due to node mobility. Potential based routing is one of the promising technologies to accomplish MANET-like routing in an autonomous manner. There have been several proposals for carrying out potential routing and autonomously exchanging potential information among nearby nodes is the common basic approach for most of these protocols. Since some time is needed until the potential information is propagated within the network, the convergence time of potential updates and assurance of node reachability are suitable indicators for the performance of these routing protocols.

Each potential routing scheme has its own benefits. However, as far as we know, none of them can deal well with situations of highly changing topology caused by geographic movement of nodes. Potential based routing is based on the field theory of physics, which is well reliable as the basis of ICT management. This mechanism is expected to improve reliability in communications on topologically fluctuated conditions, compared with mechanisms based on empirical background. Therefore, we focus on mobility oriented extensions of potential routing, called Mobility Tolerant Firework Routing (MTFR) [22], in order to improve the data transmission reachability. The potential value of a node is an indicator of its proximity to the destination and we use a broadcast based data replication scheme to improve reachability in combination with a potential threshold to limit the number of unnecessary broadcasts.

Among the first studies on potential based routing, Basu et al. [38] proposed *potential based routing* (PBR) as traffic-aware routing. The potential of each node and link

is calculated from both distance and traffic volume information with a weighting factor. The authors showed that PBR works well in a slowly varying traffic situation, but did not present any results on adaptation to dynamic traffic conditions. Following their work, several other researchers proposed variations of potential based routing.

Baumann et al. [39] proposed HEAT using anycast routing for wireless mesh networks. HEAT assumes a potential analogous to thermal conductivity. This conductivity level is exchanged with neighboring nodes and used as an indicator for traffic routing. Similarly, Lenders et al. [40] proposed link-diversity routing using the FDMR (*Finite Difference Method Routing*) algorithm, which is also based on an analogy to heat levels, but with a more lightweight potential calculation scheme than HEAT. The nodes exchange their temperatures with their neighbors and the temperature difference between source and destination node is propagated over the network. In [41] *Potential Management based Proactive Routing* (PMPR) is proposed, where nodes update their potential on demand leading to signaling cost reduction. In [42] *Parameterized Gradient Based Routing* (PGBR) is proposed, where the potential gradient is calculated in a stochastic manner using the load of links and nodes. PGBR is considered for IPTV services run by different operators on a single IP network infrastructure.

In terms of theoretical analysis, Toumpis et al. [43] proposed "packetostatics" and analyzed potential routing especially from the viewpoint of physics. They focused on traffic flows in a densely populated sensor network identical to an electrostatic field. The theoretical analysis of potential functions is discussed from the viewpoint of electromagnetic field analysis. In addition, Toumpis [44] also surveyed wireless sensor network management approaches based on analogy with physics. Moreover, Bettstetter [45] analyzed the relationship between node assignment density and graph connectivity which provides us theoretical approximations of PBR under static node placement. In addition to the physical viewpoint, *random geometric graphs* (RGGs) have been mathematically well-studied and network connectivity between nodes is represented by vertices and links. With this type of RGG model, Penrose [46, 47] and Gupta et al. [48] have estimated connectivity and critical values for drastic graph changes. Recently, Diaz et al. [49] have studied dynamic

connectivity formally in an RGG model.

As stated above, most of the potential routing methods have their benefits to achieve robustness, but usually they are assumed and evaluated in slow or non-mobile conditions. We believe that mechanisms that operate well in highly dynamic traffic conditions while improving data transmission reachability are very important for the future Internet infrastructure. As a first step to perform the above mission, we propose in our initial research work MTFR (*Mobility Tolerant Firework Routing*) [22].

In this chapter, we first investigate and reveal basic tendencies and advantages of our approach from the viewpoint of efficient wireless communication. Then, we especially pay attention to the relationship between transmission reachability and wireless coverage. The rest of this chapter is organized as follows. In Section 3.2, we first explain the basic mechanism of potential-based routing before describing our proposed firework routing mechanism in detail. Then, in Section 3.3, the performance of our proposal is compared with conventional potential routing for the random walk and random waypoint mobility models. In Section 3.4, our proposed mechanism is analyzed from a theoretical viewpoint. In Section 3.5, an extension with a self-organizing mechanism is proposed and evaluated by computer simulations. Finally, Section 3.6 concludes this chapter.

3.2 Proposal of Firework Routing Protocol

In this section, we propose our novel extension of potential routing to improve node connectivity. First, we discuss conventional potential routing with the example of link-diversity routing. Then we introduce our proposed mechanism and discuss protocol details.

3.2.1 Conventional Potential Routing

We now explain conventional potential routing for the example of link-diversity routing [40]. This routing scheme is based on a thermodynamic analogy and a typical network model is shown in Figure 3.1.

When the source attempts to establish a connection to the destination, it broadcasts

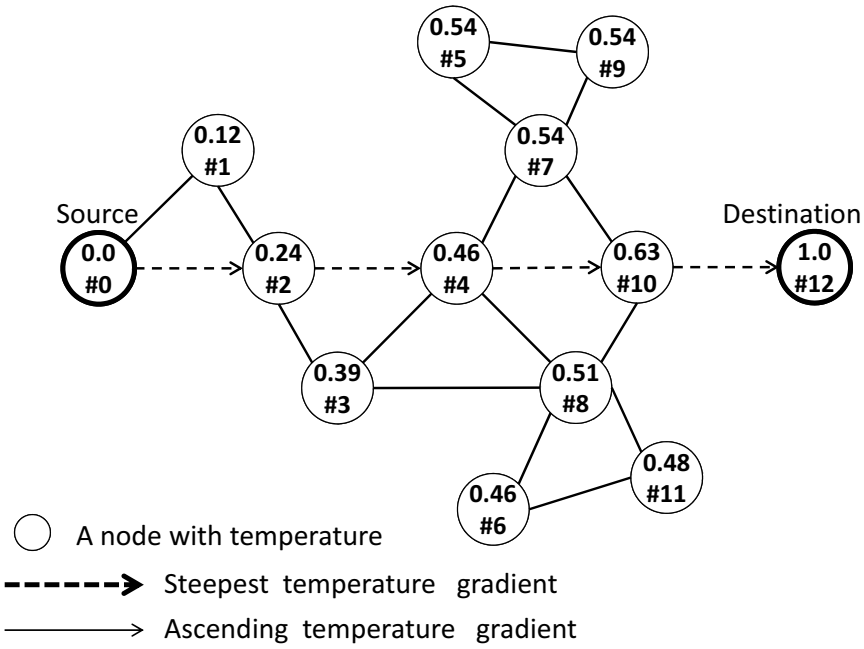

Figure 3.1: Example in conventional potential routing (link-diversity routing)

a route request to its neighbors which forward the requests in a flooding manner until the destination node is found. Each node has its own *temperature* parameter that is iteratively calculated as average of its neighbors' temperatures and exchanged among neighbor nodes.

$$\phi_{t+1}(x_i) = \begin{cases} \frac{\Sigma_{k \in nbr(x_i)} \phi_t(x_k)}{|nbr(x_i)|}, & |nbr(x_i)| > 0 \\ 0, & |nbr(x_i)| = 0 \end{cases}$$

where the network has the set of nodes $\{x_1, \cdots, x_n\}$, the set of neighbor nodes of x_i is expressed as $\{x_k; k \in nbr(x_i)\}$, and ϕ_t indicates the temperature of x_i at iteration step t. In addition, the temperature of the source node x_s and destination node x_d are constant and have their own boundary conditions as $\phi_t(x_s) = 0$ and $\phi_t(x_d) = 1$, $\forall t \geq 0$. After convergence of the temperature calculation, each intermediate node forwards packets toward its neighbor node which has the highest temperature. As a consequence, packets sent from the source node will reach the destination node along the steepest temperature gradient

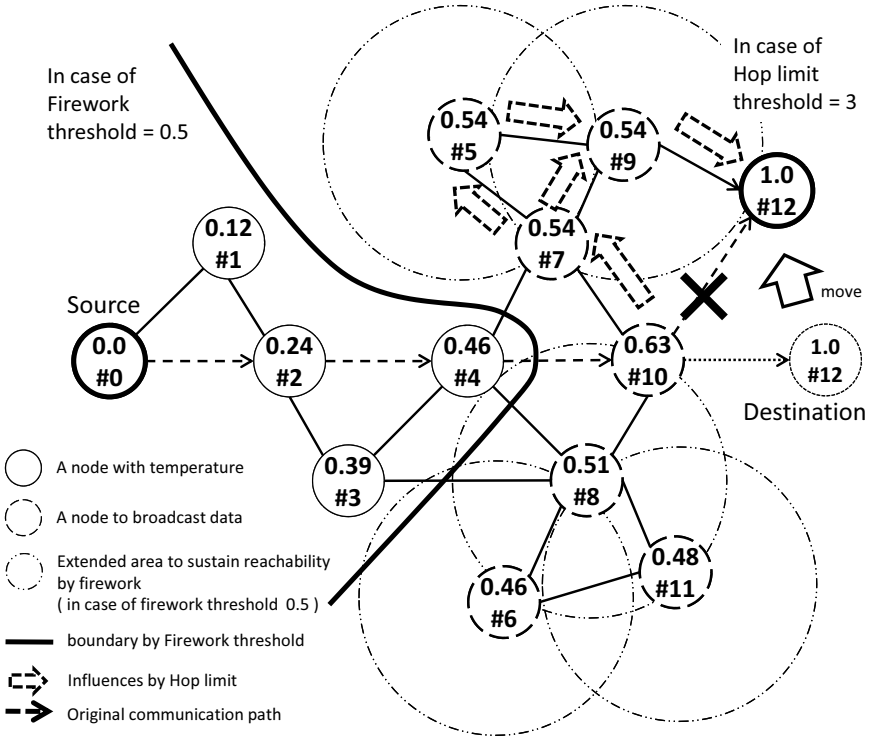

Figure 3.2: Explanation of proposed MTFR

path as shown in Figure 3.1.

While this method is effective for static nodes, it faces problems under dynamic conditions. Depending on the network size, many iteration steps are required until the temperature potential, i.e. the correct route to the destination node, has converged. Thus, each time a potential is calculated, it is only valid for the period of time when the topology does not change. If the destination node leaves the transmission range of its last hop node, the correct route can not be found and a new flooding of the entire network is required to update the potential. In our MTFR method, which will be described in the following section, we improve this behavior by restricting the nodes that are involved in the broadcast process.

3.2.2 Mobility Tolerant Firework Routing (MTFR)

In our proposal, we introduce two additional parameters, *firework threshold* and *firework hop limit*, to faster react in situations when the destination node becomes unreachable. We assume that if the destination node moves away from its last position, it will be most likely located somewhere nearby. Since the temperature can be regarded as a relative distance of a node to the destination, the firework threshold is used to limit the broadcast in search for the destination to only nodes in the previous vicinity of the destination. If the temperature is below the firework threshold, the node only forwards data packets and if it is above, it broadcasts them. In order to further reduce overhead, broadcasts are only replicated up to the firework hop limit. This scheme is effective not only for the destination node's movement but also for intermediate node movement. In the case of an intermediate node's movement, our method also reinforces disconnected links by broadcast and the two threshold parameters provide us with sufficient adjustment.

Figure 3.2 shows a simple network example with MTFR. As an example, the destination node is assumed to be moving in the direction of the solid white arrow. After the movement, the original last hop link between the destination and node #10 with temperature 0.63 becomes disconnected and hence conventional potential routing would fail in such a situation. On the contrary, with MTFR node #9 with temperature 0.54 broadcasts packets to all of its neighbors and therefore packets will continue reaching the destination via node #9 without recalculation of all nodes' temperatures. We define two parameters for our firework routing as firework threshold and hop limit, which can control how long and how wide firework effects will be, respectively.

3.2.3 MTFR Protocol

For an actual implementation of MTFR, we need to confirm that temperature exchange with neighbor nodes, temperature update harmonized with neighbor nodes, and packet forwarding according to temperature are feasible. The protocol sequence is described in

```
1: Power on the device
2: Node initialization procedure
3: Establish links with neighboring nodes
4: Initial temperature calculation with all nodes before in-service
5: Collection of call condition
6: Call origination procedure
7: for communication time= 1, 2, ..., end time do
8:    if condition timer has expired then
9:       Collection of call condition
10:      Adjust "temperature update timer" according to status
11:      Adjust "hop limit number" according to status
12:      Adjust "condition update timer" according to status
13:   end if
14:   if temperature update timer has expired then
15:      for active link number= 1, 2, ..., n do
16:         Collection of TheirTemperature from all the neighbor nodes
17:         if any of TheirTemperatures has changed then
18:            Update MyTemperature
19:         end if
20:         if MyTemperature has changed then
21:            Send new MyTemperature
22:         else if MyTemperature is unchanged then
23:            Send short message to indicate "no-change"
24:         else
25:            System status failure
26:         end if
27:         Receive TheirTemperature message
28:      end for
29:   end if
30:   if there is a packet to be forwarded then
31:      if MyTemperature is greater than firework threshold then
32:         Broadcast packet to all the neighbors
33:      else if MyTemperature is less than threshold then
34:         Forward packet to highest temperature neighbor
35:      end if
36:   end if
37: end for
38: Call termination procedure
```

Figure 3.3: Firework routing protocol algorithm

pseudocode in Algorithm 3.2.2 and mainly consists of three parts: system parameter revision procedure, temperature update procedure, and packet forwarding procedure. From Algorithm 3.2.2, preparations for in-service by a mobile node are done (lines 1-5) and communication is started (line 6). During the call busy state, the mobile node operates mainly three tasks periodically (line 7). First, the mobile node maintains several system management timers to update system parameters such as temperature update timer, hop limit update timer, and system condition timer. After the system condition timer expires, the mobile node adjusts each system parameter value at the right time (line 8-13). Second, if the temperature update timer expires, the mobile node starts temperature recalculation (line 14). Concerning each active link with neighbor nodes, their temperature values are collected (line 16) and the node's own temperature is recalculated with them (line 17). If its own temperature has changed after recalculation, the mobile node sends the new temperature to all the neighbor nodes (line 21) and if not, a short notification message indicating no change is sent (line 23). On the other hand, updated temperature messages from neighbor nodes are also received (line 27). Each node can utilize the sequence number in exchanging temperature messages for avoiding confusion among each node's update timing gap. Third, the mobile node looks up the packet transmission table and sends packets to appropriate neighbor nodes according to its own temperature value (line 30). If the temperature is above the firework threshold, the packet will be sent to all neighbor nodes with greater temperature than its own (line 32) and if the temperature is under the firework threshold, the packet will be sent to the single neighbor node with the highest temperature (line 34). Several broadcast algorithms can be considered and another threshold can be defined to select nodes to broadcast packets. Finally, the mobile node terminates the call (line 38).

3.3 Numerical Evaluations

In this section, we evaluate our proposed method by simulations using the random walk (RWK) and random waypoint (RWP) mobility models for nodes distributed initially in a uniform random way. In RWP constant motion speed and no pause time are assumed.

Table 3.1: Basic simulation parameters in evaluations of MTFR

Parameter	**Value**
Initial network layout	uniformly random in 10km x 10km area
Number of nodes	2000 – 4000
Wireless range	100 – 500 m
Speed of mobile node	1 m/s (pedestrians) 20 m/s (cars) 100 m/s (bullet trains)
Firework hop limit	7 hops
Firework threshold	0.5
Mobility model	RWK RWP (const. speed, no pause)
Simulation time	100 – 300 sec

Basic simulation parameters are listed in Table 3.1. Each simulation result is based on the average of hundred or more samples, so we omit showing confidence intervals. If not mentioned otherwise, the number of nodes is 4000, mobile speed is 100 m/s, firework hop limit is set to 7 hops, firework temperature threshold is 0.5, and simulation time is 100 sec.

3.3.1 Effects of Wireless Coverage

In this section, we investigate the basic tendency of the firework effect on the influence of packet reachability with number of nodes and wireless transmission range. From Figure 3.4, we can conclude that the packet reachability improves with the number of nodes and with the transmission range. This is because increasing both values results in a wider wireless coverage area. MTFR is able to restore reachability almost completely to that of theoretically maximum possible without mobility. Wireless transmission range affects node density with an exponent of 2, which produces a stronger relationship with reachability. Therefore, steeply increasing curves are observed.

It was also observed that there are some unrecoverable conditions in certain densely populated cases like 4000 nodes and over 400 m wireless ranges. Here, firework improvement effect corresponds to the reachability difference between results obtained with and without firework. This is because the increase of possible links with more neighbors has the side

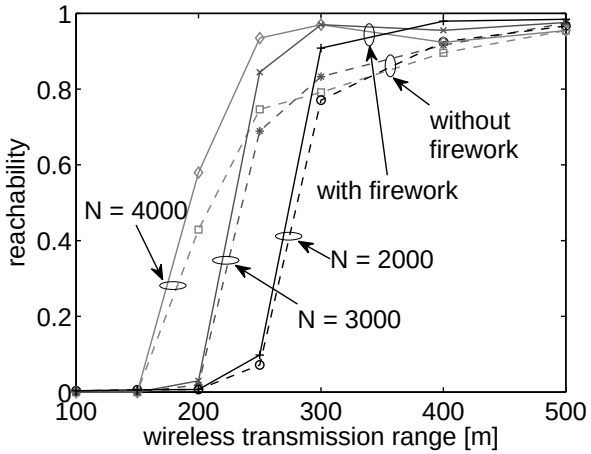

Figure 3.4: Influence of transmission range on reachability

effect of increasing the hop counts, which eliminates the firework effect by the hop number limit. In conclusion, there is an optimal point against the number of nodes and wireless transmission range on reachability improvement under some specific conditions.

3.3.2 Impact of Vehicular Speed

We also investigate the tendency against mobile node speed. Figure 3.5 shows that for speeds less than 20 m/s no firework effects are observed. The curves for 1 m/s are not shown here as they coincide with those for 20 m/s speed. However, for higher speed of 100 m/s quite large effects of around 0.2 improvement compared to without firework begin to appear. The reason for this lies in the increased vehicular speed, which produces on average larger movement distances. Therefore, the higher the mobile node's speed is, the larger the firework effects are.

3.3.3 Influence from Node Mobility Model

Next, we analyze the influence of the mobility model on our method using RWK and RWP. The improvement in reachability by firework method is shown in Figure 3.6. In the case of RWK, almost no effect can be seen by firework, but significant improvements by firework

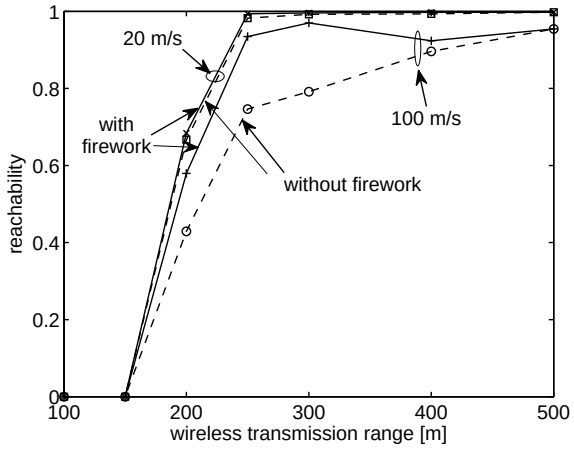

Figure 3.5: Influence of vehicular speed on reachability

are observed in the case of RWP even at the speed of 1 m/s irrespective of the number of nodes.

This tendency has a relationship with average movement distance by mobile nodes. The traversed distance is larger in RWP than RWK due to its directional movement, and therefore the probability becomes higher to get out of reach of wireless coverage. In order to compare average movement distance in both random walk mobility and fixed one directional walk (ODW) mobility, it has been reported [50] that the average distance of each movement $w_{\mathrm{RWK}}(t)$ and $w_{\mathrm{ODW}}(t)$ after time t passed can be expressed as $E\left[w_{\mathrm{RWK}}(t)\right] = \sqrt{t}$ and $E\left[w_{\mathrm{ODW}}(t)\right] = t$, where ODW implies the motion that mobile nodes move in a straight-line with constant speed, which is comparable to the ideal case of the random waypoint mobility with no pause time. Therefore, from the above two equations, it can be concluded that movement in RWK generates less average movement distance than RWP. As a consequence, reachability improvement in RWP becomes larger than in RWK.

3.3.4 Effects of Temperature Update Time Interval

In this section, we show the simulation results for different simulation time. Figure 3.7 shows when simulation time is 100, 200, and 300 sec with 4000 nodes at the speed of 1 m/s

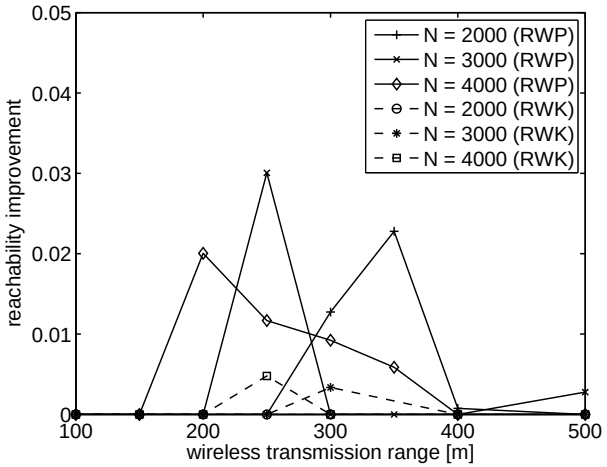

Figure 3.6: Reachability improvement under different mobility models

under RWP. Here, reachability improvement is defined as difference in reachability between with firework and without firework. Since we adopt a sufficient convergence threshold value to quickly restore the perfectly recovered state after temperature convergence, the simulation time is equivalent to the temperature update time interval. This equivalence is explained by considering repeated simulations and temperature calculation by turns. From Figure 3.7, the increase of temperature update time interval results in larger firework effects. This is due to the same reason of increasing communication opportunities explained in Section 3.3.1.

3.3.5 Evaluation of Transmission Delay

Figure 3.8 shows simulation results of end-to-end transmission delays per a packet transmission generated with different numbers of nodes under RWK at the speed of 20 m/s and with different ranges for packet transmission. Here, end-to-end delay means the average number of hops traveled by a transmitted packet from the source node to the destination node. In addition, the difference of end-to-end delay is the discrepancy in delay between with firework and without firework. In smaller wireless ranges, transmission delays are observed as almost zero in all conditions due to lack of reachability and in addition, in

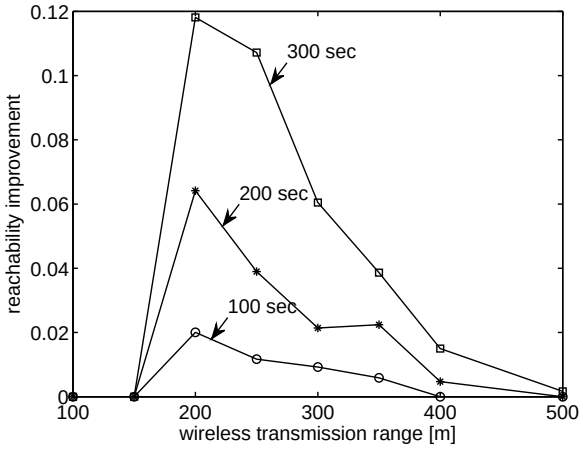

Figure 3.7: Reachability improvement over temperature update time interval

larger wireless ranges, delays are converged to around 15-20 hops in all conditions due to almost full reachability. However, in middle wireless ranges, we can recognize some additional transmission delays due to the firework procedure. However, from Figure 3.8, it turned out that delay differences between results with and without firework were limited to less than 6 hops in all cases. This fact indicates that our MTFR is feasible enough for real communication scenarios. As a result, MTFR produces better reachability at the expense of a small additional transmission delay from overall viewpoint.

3.3.6 Evaluation of Traffic Overhead

In addition, we analyze the tendency from the viewpoint of traffic overhead accompanied by the firework procedure. Figure 3.9 shows simulation results of additional traffic overhead by firework with different numbers of nodes under RWK at the speed of 100 m/s and with different wireless ranges for packet transmission. Here, traffic overhead is defined as the total number of hops traveled by transmitted packets and normalized by the number of nodes and total amount of reachability recovery. From Figure 3.9, in higher wireless transmission ranges such as more than 350 m, it is shown that there is no much difference between without and with firework. On the other hand, in the middle wireless transmission

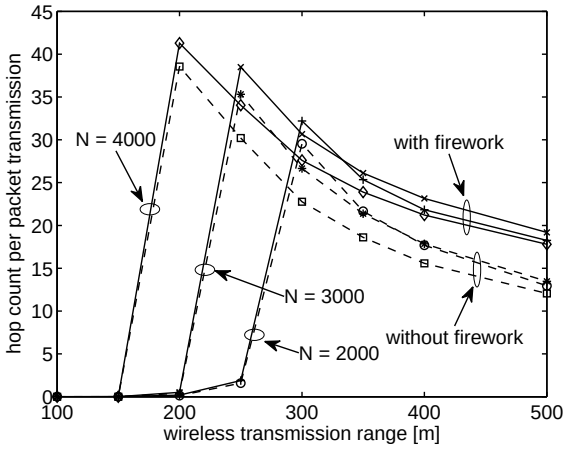

Figure 3.8: Transmission delay analysis

ranges from 200 m to 350 m, additional traffic overhead by firework is observed but they are less than 3.5 hops. In addition, in lower wireless transmission ranges such as less than 200 m, there is no difference between without and with firework due to poor reachability in both cases. Even though firework routing requires in the medium range cases additional traffic overhead, reachability recovery has more importance over overhead increase for the future network infrastructure, since it allows a connection to the destination compared to without firework. Moreover, here in our simulation, we use a fixed firework threshold 0.5 and the higher firework threshold we utilize, the less additional traffic overhead is produced. We can also easily embed some additional intelligence to reduce the overhead by avoiding unwanted replicated packets, for example, by not broadcasting packets to nodes that have a low expectation of recovery due to their temperature or vehicular motion. As a consequence, the above results can be seen as worst case scenario and indicates that firework inevitably produces an increase of traffic overhead to some extent, but the benefits of higher connectivity with MTFR outweigh this drawback to make it feasible enough for an actual system implementation.

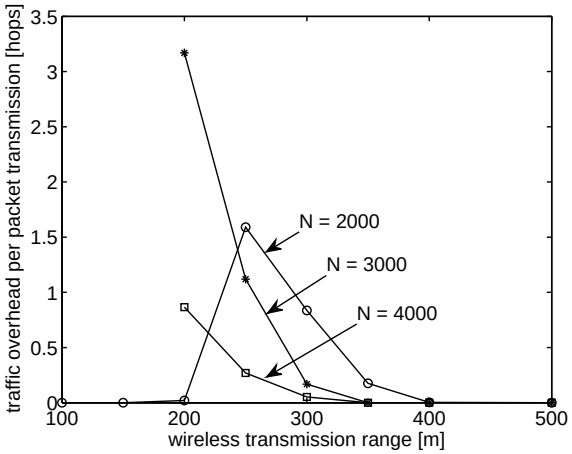

Figure 3.9: Traffic overhead analysis

3.3.7 Improvement Analysis by Firework Routing

In this section, we analyze the improvements achieved by the firework method in terms of reachability, end-to-end delay, and traffic overhead.

First, Figure 3.10 shows simulation results of reachability improvement by firework with different numbers of nodes under RWK at the speed of 100 m/s and with different wireless ranges for packet transmission. In smaller and larger wireless transmission ranges, reachability improvement is almost zero due to lack of connectivity and no room for recovery, respectively. On the other hand, in middle ranges, there is a peak for each curve in which wireless range is on the increase as the number of nodes decreases. In addition, the maximum value slightly decreases as the number of nodes decreases, and therefore, like in Section 3.3.1, the wireless range has larger effect on producing full reachability than the number of nodes.

Second, Figure 3.11 shows simulation results of end-to-end delay increase per packet transmission generated with different numbers of nodes under RWK at the speed of 100 m/s and with different ranges for packet transmission. In smaller and middle wireless transmission ranges, the tendency of maximum delay increase shows similar results as those of reachability. However, in larger wireless transmission ranges, degradation is saturated at

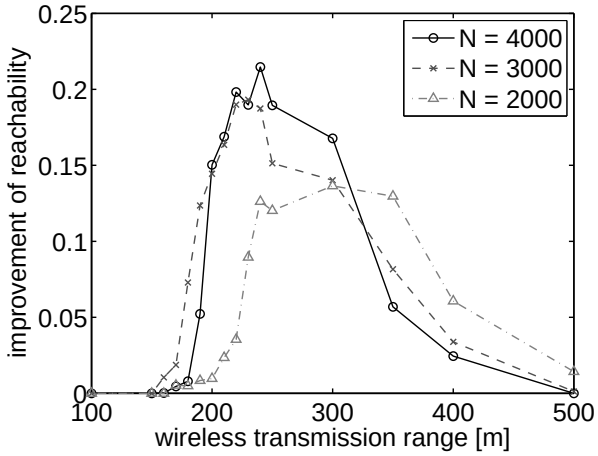

Figure 3.10: Reachability improvement analysis

the level of almost 5 hops. This is because the temperature gradient sustains the basic principal communication route on one side, but it doesn't allow shortcut routes on the other side. Hence, it produces some fixed delay.

Third, Figure 3.12 shows simulation results of additional traffic overhead increase by firework with different numbers of nodes under RWK at the speed of 100 m/s and with different wireless ranges for packet transmission. In smaller and larger wireless transmission ranges, the overhead increase is almost zero for the same reason as in reachability improvement analysis of this section. The wireless range for each maximum overhead peak shifts similarly from small range to large range.

3.3.8 Firework Parameter Study

Finally, we analyze parameter influences by the firework method. Figures 3.13 and 3.14 show simulation results of reachability improvement by firework with different hop limit and firework threshold values, respectively, which are simulated for 3000 nodes under RWK at the speed of 100 m/s and with different wireless ranges for packet transmission. From Figure 3.13, 4 hops might be the best for high reachability and less overhead to some extent. It is observed that the best hop limit value depends on current conditions such as node

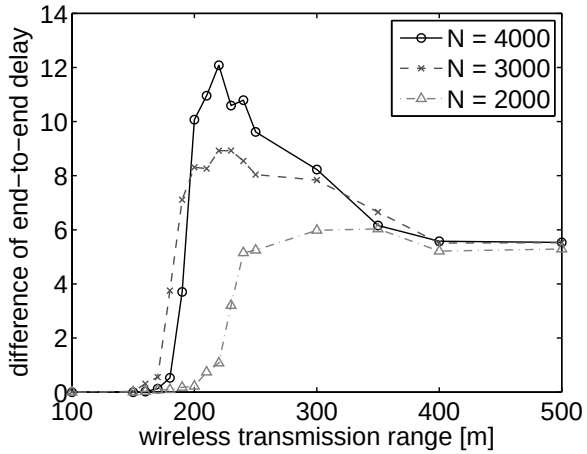

Figure 3.11: Difference of end-to-end delay per packet transmission

density. In addition, from Figure 3.14, it is shown that firework threshold value should be selected in more precise manner than hop limit value. For example, the firework thresholds between 0.5 and 0.7 might be the best parameters in case of wireless transmission ranges 250 m, 300-350 m, and 400 m or more, respectively.

Now that we understand that firework parameters should be selected carefully according to current conditions, we develop an autonomous parameter adaptation mechanism in Section 3.5. Same as for the hop limit cases, it is observed that the best firework threshold value varies depending on current conditions such as node density.

3.4 Theoretical Analysis

In this section, we add a theoretical analysis on connectivity in gradient-based routing to verify our simulation results. First, we define the network model. A set of n nodes are independently randomly placed on an area A, each with a certain wireless transmission range r. We assume that the simulation area is large enough for us to consider a constant node density $\rho = n/A$.

In order to calculate the probability of graph connectivity, we use nearest neighbor methods [45]. The probability density function of the nearest neighbor distance ξ is expressed

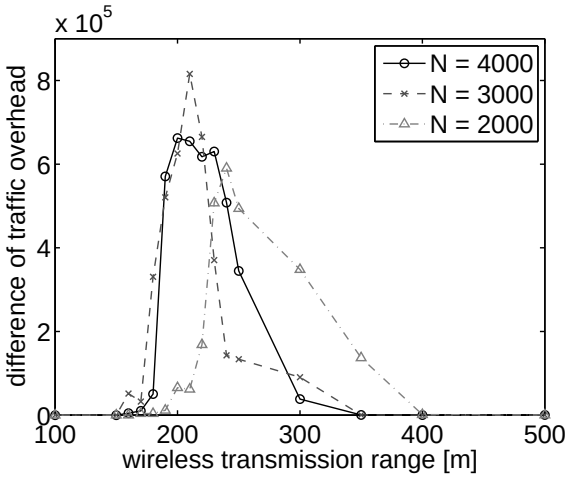

Figure 3.12: Traffic overhead degradation analysis

as

$$f(\xi) = 2\pi\rho\,\xi\,\exp(-\rho\pi\xi^2) \qquad \text{for } \xi > 0. \tag{3.1}$$

In addition, the probability that a randomly selected node has its nearest neighboring node with less than or equal to the wireless range r is calculated as

$$P(\xi \leq r) = \int_0^{\infty} f(\xi)\,d\xi = 1 - \exp(-\rho\pi r^2). \tag{3.2}$$

With the above equation, the probability that a node x is isolated and has no neighboring node can be calculated as

$$P(g(x) = 0) = P(\xi > r_0) = \exp(-\rho\pi r_0^2) \tag{3.3}$$

where, $g(x)$ indicates the number of neighboring nodes of a node x. As a consequence, we

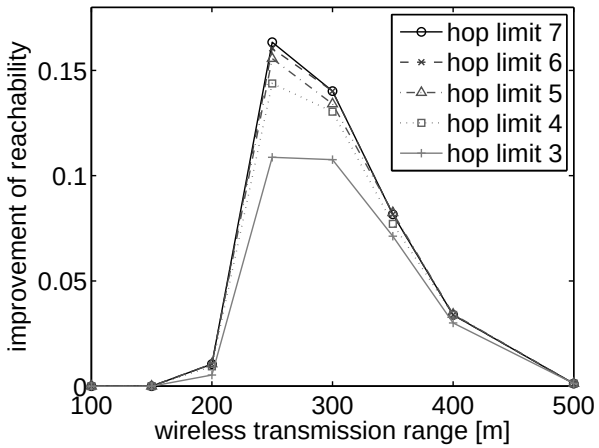

Figure 3.13: Reachability improvement versus hop limit

can get the following probability that all nodes are connected.

$$\begin{aligned} P(g_{min}(x) > 0) &= \binom{n}{n} P(g(x) > 0)^n \, P(g(x) = 0)^0 \\ &= \left(1 - \exp(-\rho\pi r_0^2)\right)^n \end{aligned} \tag{3.4}$$

This is the probability of connectivity among nodes and is stricter than the connectivity between randomly selected source and destination node. From Equation (3.3), each node has an expected number of neighbors $E(g) = \rho\pi r^2$. Therefore, the average component size that a randomly selected node belongs to is approximated by the sum of the terms of the geometric sequence

$$\begin{aligned} \langle s \rangle &= \rho\pi r^2 + (\rho\pi r^2 - 1)^2 + (\rho\pi r^2 - 1)^3 + \cdots \\ &= \frac{B\left(1 - B^k\right)}{1 - B} + 1 \end{aligned} \tag{3.5}$$

where $B = \rho\pi r^2 - 1$ is the term in the geometric series and k is the depth of neighboring nodes taken into consideration. With Equation (3.5) we can then give the probability of

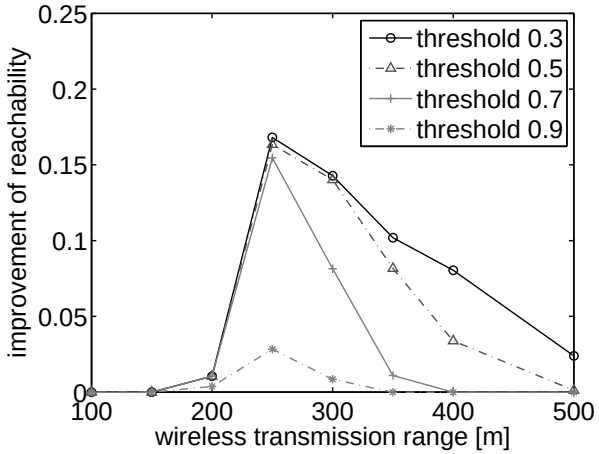

Figure 3.14: Reachability improvement versus firework threshold

connectivity P_c as in Equation (3.6).

$$P_c = \frac{\langle s \rangle}{N} \frac{\langle s \rangle - 1}{N - 1} \tag{3.6}$$

Figure 3.15 shows a comparison between theoretical and simulation results with $k = 5$ under 3000 nodes distribution. From Figure 3.15, theoretical and simulation results agree to each other in all the conditions with different wireless transmission ranges. We also confirm that the above equation works well with different number of nodes (not shown here).

3.5 Consideration of Parameter Adaptation Mechanism

In this section, we formulate some thoughts about extending our MTFR into a self-organizing system. Figure 3.16 shows a state diagram of an MTFR-based self-organizing system. Basic states of the system consist of *Firework phase* and *Lock-in phase*. Firework phase appears on the condition that the firework routing is in operation due to the loss of original communication paths. On the contrary, Lock-in phase appears on the condition that the firework routing causes more additional overhead due to an active original communication path. Firework phase is divided into two modes, *deterministic mode* and *Yuragi mode*, depending

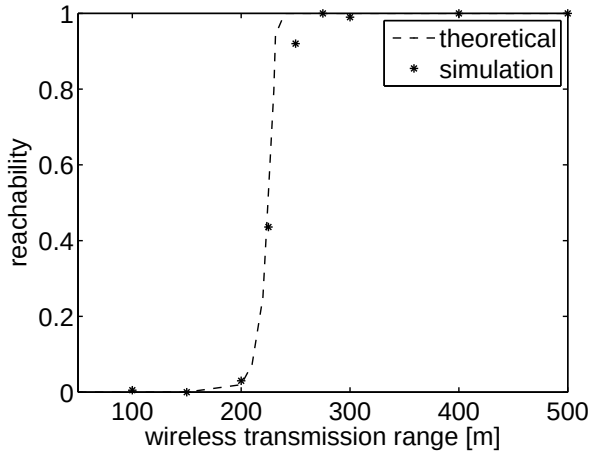

Figure 3.15: Theoretical analysis in static mode

on the presence of links from the neighboring node to the destination node.

In deterministic mode, the destination node has a certain number of links to one of its neighboring nodes and the system adjusts the firework threshold and the hop limit at every specific time step according to the destination node's motion. For example, if the destination node is approaching one of its neighboring nodes toward the source node, then the firework threshold and the hop limit values will be changed into more loose ones in order to avoid unnecessary traffic overhead. On the contrary, if the destination node is receding, then the two parameters will become more strict in order to achieve higher reachability.

On the other hand, in Yuragi mode, the destination node has no links to its neighboring nodes and parameter management by the system will not have any influence on system performance and additionally will increase management cost. Therefore, it should follow a management procedure on a random basis to avoid unnecessary management cost increase.

Figure 3.17 shows that simulation results of reachability in the self-organizing system with 3000 nodes under RWK at the speed of 100 m/s and with different ranges for packet transmission. In this simulation, each step size to update firework threshold value and hop limit value adaptively is 0.05 and 0.5 , respectively. From Figure 3.17, it is confirmed that our proposed self-organizing mechanism is capable of extending improvement of reachability.

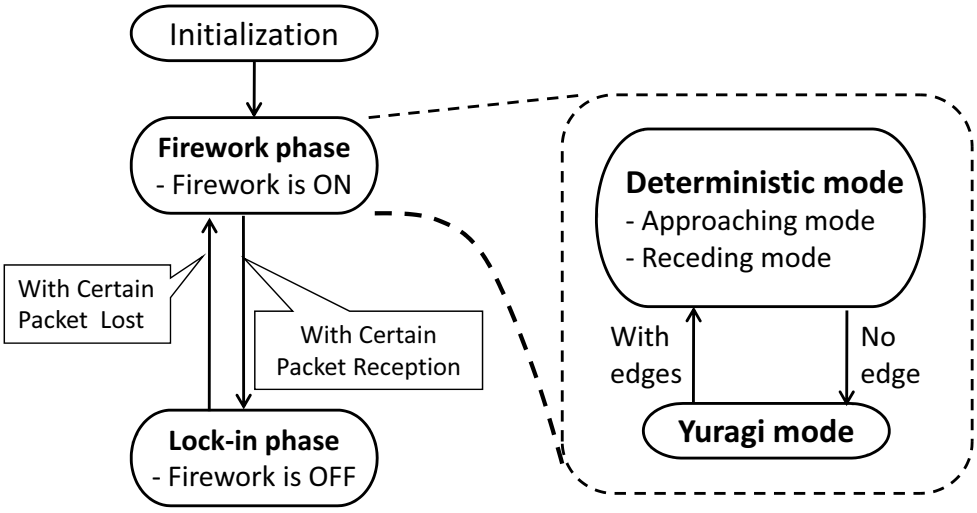

Figure 3.16: State diagram of self-organizing mechanism

We have just started with our investigation by a basic model to construct a self-organizing system. However, the principal components of our mechanism seem to be similar as those of biologically inspired mechanisms, such as the attractor selection mechanism [51], from the viewpoint of switching between deterministic and random modes depending on the environment. Therefore, our future goal is to compare our proposed method with biological methods.

3.6 Conclusion

In this chapter, we proposed a novel mobility assisted firework routing mechanism named Mobility Tolerant Firework Routing to improve packet reachability and we evaluated it by simulations with the the random walk mobility model. In addition, we added a theoretical analysis and proposed an extension to a self-organizing system and evaluated it by simulations.

First, we studied the performance of our method from the wireless coverage viewpoint. It turned out that our method showed a good improvement in reachability by the firework effect and the increase in wireless coverage resulted in general in a higher reachability.

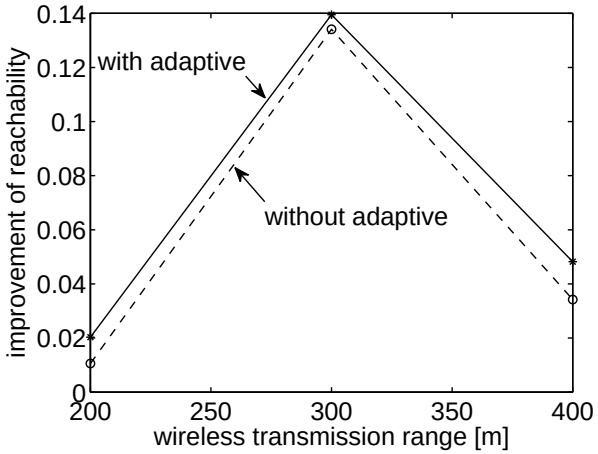

Figure 3.17: Simulation results in self-organizing system

Next, we analyzed the improvement by firework from the viewpoint of packet reachability, end-to-end delay, and traffic overhead. On all the conditions, it was confirmed that there were large reachability improvements while having slightly additional transmission delay and traffic overhead. The most suitable condition to produce maximum reachability and lowest traffic varied according to the given conditions. Third, we analyzed two parameters, firework threshold and hop limit against packet reachability. We also confirmed that the best values for both parameters exist and they varied depending on system conditions such as wireless transmission environment.

In addition, we performed a theoretical analysis from the viewpoint of connectivity for random node distribution. We formulated an equation to express packet reachability and it was confirmed that theoretical results obtained by our formula matched simulation results well. Finally, we proposed an extension of MTFR to a self-organizing system. Simulation results showed that our extended MTFR achieved higher reachability than that generated by simple MTFR.

From the above discussion, we confirmed that our method produces improved reachability at the expense of a small additional transmission delay and traffic overhead and we believe that our proposed method is feasible and achieves higher reachability than standard flooding. Additionally, by extending the methods with an adaptive parameter management

system, we consider MTFR to have the ability to further improve reachability and can become a better candidate for a safe and secure social communication network infrastructure. As an extended evaluation for our further study, we are also interested in investigating link sustainability when mobile nodes move.

Chapter 4

Future Mobile Network Management With Attractor Selection

Several task forces have been working on how to design the future Internet and it is high time for research work to move a step forward to networks on a large scale. In this chapter, we propose an future mobile network architecture on a combination of OpenFlow and the attractor selection method to achieve scalability and energy saving. In addition, we propose novel wireless network management concepts on the extension of the attractor selection mechanism that achieves energy saving from the viewpoint of route calculation and signaling cost. First, we propose a concept to select the best suited interfaces for mobile nodes depending on instantaneous live traffic volume. Then, a concept to define the best clustering domain is proposed to effectively reduce handover signaling cost. Through the above, our proposed architecture is a good candidate as the future mobile network.

4.1 Introduction

From the viewpoint of user needs for our future society, the wireless communication environment is essential, and as research activities for wireless future network research, there have been several research activities such as the MobilityFirst Project [4] of the FIA program and POMI (Programmable Open Mobile Internet) 2020 of Stanford Clean Slate Program. In addition, there are several architectures suitable for the future mobile network with separated identifier and locator [5]. Among these activities, one of the most promising future Internet research activities is OpenFlow technology [6] to construct a programmable and environmentally-friendly ICET infrastructure [7–9]. The OpenFlow technology has a potential to meet a wider variety of requirements from users due to its programmability and OpenFlow is available not only for wireless communication but also for wired. However, the above researches are limited within local sites such as campus networks and data center networks for the time being.

In addition to mobility support, robustness is one of the keywords when talking about the future Internet infrastructure for coping with disasters like huge Tsunami or earthquakes. In addition, energy saving for protection of the environment is also an important factor. To achieve the above targets, more reliable infrastructures based on theoretical background are desired instead of approaches based on empirical background. For instance, biological systems have evolved over a long period of time and have a robustness against environmental changes, which helps in the survival of the species. For this reason, there have been recently several mechanisms based on biological systems applied to future ICET [52–54]. Among biologically-inspired control mechanisms, attractor selection is one of the possibilities to formulate a mathematical model based on biological dynamics. Recently, there have been several research activities applying the attractor selection method to ICET management field in Yuragi Project [17] and in the Global Center of Excellence Program for Founding Ambient Information Society Infrastructure [18].

The current Internet has been evolved to maintain a backward compatibility by adding new functions whenever they are needed. However, it was come to a conclusion that the new

future Internet infrastructure should be rebuilt from scratch. One key technology for the future Internet is network virtualization established by programmable network components based on OpenFlow technology [7]. As an essential fraction of the future Internet, Yap et al. [8] draw a blueprint for future wireless mobile networks that can achieve handovers between WiMAX and WiFi environment. In addition, Yap et al. [9] deployed a testbed named as the OpenRoads to offer a slicing service in wireless infrastructure on a campus network. Here, this slicing service means that shared common wireless resources can be offered to users in a flexibly separated manner with a finer granularity.

In its original context within biological systems, Kashiwagi et al. [55] formulated a mathematical model of attractor selection to express an adaptive response system through differential equations. In this model, the dynamics of gene expression in E. coli cells are described in terms of the environmental changes of nutrient conditions. In addition, Furusawa et al. [56] introduced another attractor selection model based on adaptability between gene regulatory network in a cell and metabolic network. For both models, noise is one of the important factors. Once the system is settled down to an attractor, the system should stay at the same attractor until the condition becomes unsuitable. On the other hand, if the condition becomes unsuitable, the system should move and find the other better attractor. The activity locks the system to stay at the same attractor and noise works for offering the trigger to find the other attractor. Based on the above models, Murata et al. [18] developed and extended ambient network management to give birth to future human life closely related to environmental adaptability, which is a part of the activities of GCOE (Global Center Of Excellence) program. Within the Yuragi Project [17] and the GCOE program, several research activities have been produced.

Additionally, from a theoretical viewpoint, Leibnitz et al. [57] extended the above Kashiwagi-model into multi-dimensional control mechanism and showed an instance of attractor selection application to multi-path routing in ad hoc networks. Wakamiya et al. [58] surveyed a wide variety of biologically-inspired systems and built a scalable architecture focusing on systems running in a self-organizing or autonomous manner based on the attractor selection. Leibnitz et al. [51] analyzed the perturbation effects in attractor

selection based on observations of the system's responsiveness to inherent fluctuations.

From an application viewpoint, Kajioka et al. [59] adapted an attractor selection model into multi-interface selection system using several wireless media such as LTE, WiMAX, and WiFi with different communication capabilities. They built a simple testbed of their model and evaluated the advantages and feasibility. Koizumi et al. [60] adapted an attractor selection mechanism into virtual network topology construction. The best overlay network topology at each moment is selected according to the outputs of the attractor selection equation.

The future mobile network and the attractor selection method have so far been well-investigated independently. However, the combination of both is not mature enough. In this chapter, we extend the above attractor selection mechanism in order to work on large-scaled mobile wireless network environments based on OpenFlow technology. First, we discuss the future mobile network on a basis of combination of OpenFlow technology and the attractor selection method. Second, we propose a method for a mobile node to select the best radio interfaces according to environmental conditions with attractor selection using an activity driven by realtime user traffic volume. Third, we establish an appropriate clustering method to reduce handover signaling cost on the OpenFlow based future mobile network with the attractor selection using an activity driven by the difference of the flow directions between user traffic and signaling traffic. Finally, we evaluate our proposed multi-radio interface selection mechanism by computer simulation. Simulation results show that our proposed mechanisms are feasible enough to work just by natural noise irrespective of an additional artificial noise as conventionally done. The rest of this chapter is organized as follows. In Section 4.2 we explain the basic mechanism of attractor selection in detail. Then, in Section 4.3, we discuss an adaptation of an attractor selection method into the OpenFlow based future mobile network. In Section 4.4, novel concepts to adopt attractor selection mechanism into the Future mobile network environment are proposed and discussed in detail. In addition, in Section 4.5.2, simulation results are explained. Finally, Section 4.6 concludes this chapter.

4.2 Basic Attractor Selection Model

This section introduces a basic attractor selection model based on ARAS (Adaptive Response by Attractor Selection) [55]. The basic model is expressed as follows:

$$\frac{dm}{dt} = f(m) \times \alpha + \eta \tag{4.1}$$

where function f is defined by the potential and a function of the state m, $0 \leq \alpha \leq 1$ is an activity of the selected attractor, and η is noise term. At each time step, one attractor is selected based on the output of Eqn. (4.1). Here, the function f defines the attractors, e.g. if we would like to define an attractor $m = 0$, then $f(m) = -m$ is one example of function f. The activity α indicates suitability of the selected attractor to the current environment. The more suitable the attractor is, the larger the activity becomes. Hence, in case of larger α, deterministic function f is dominant over noise to find an attractor. On the other hand, in case of smaller α, the random term η becomes dominant. Changes of environmental conditions reflect on the change of activity α appropriately for controlling the system. Hence, depending on the transition of activity α, both deterministic dominant and random dominant states are switched over well suited for reducing unnecessary management cost and pursuing the utmost performance. In the end, this attractor selection procedure is an effective way to adaptive system construction against environmental changes.

4.3 Proposal of Future Mobile Network Architecture

In this section, we will discuss our vision of a future mobile network architecture. We focus on a network based on OpenFlow due to many of its strong points. However, OpenFlow also has some drawbacks. First, energy cost for path calculation increases in return for flexible path establishment. Second, traffic overhead caused by frequent handovers increases because an OpenFlow controller has its own local domain and is not suitable for a large scale network as it is. Hence, we introduce an attractor selection method to improve the above drawbacks.

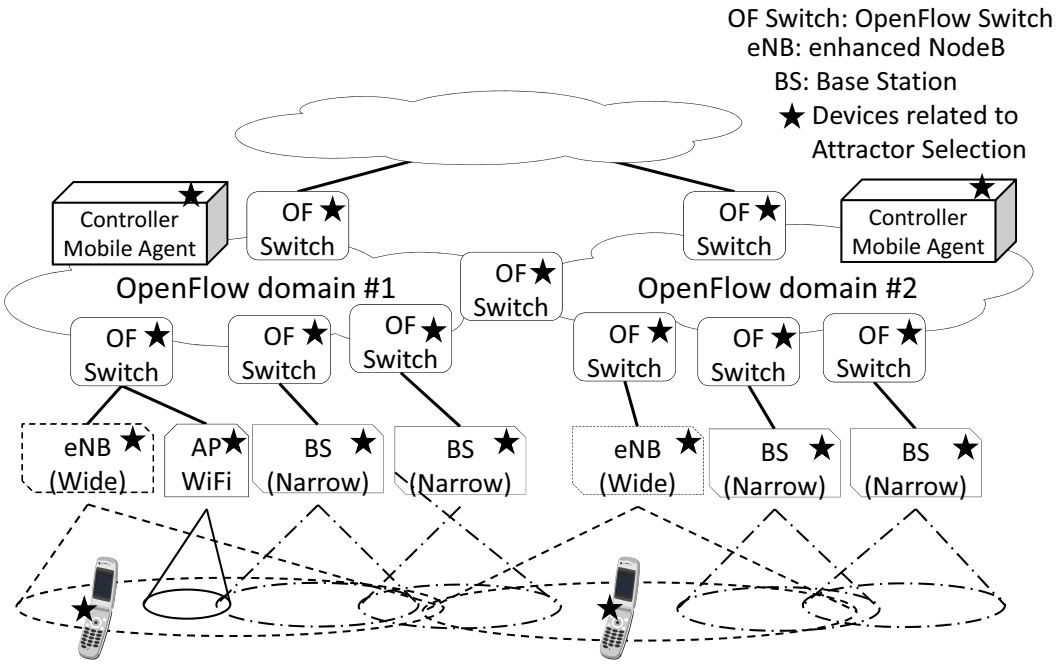

Figure 4.1: An example of future mobile wireless network

Both OpenFlow and attractor selection have been innovated and evolved independently recently and we propose a hybrid system with both technologies. Attractor selection was explained in Section 4.2. OpenFlow is a technology where centralized controllers can control user data paths of all network devices such as switches, routers, and base stations through an external standard API. In addition, data packets are handled on a flow basis, and therefore, flexible data path arrangement is possible. However, the centralized basis gives cause for worries of scalability.

Hence, we propose a future mobile network architecture taking into account both flexibility of OpenFlow and robustness of attractor selection. Our proposed architecture is shown in Figure 4.1. In this architecture, OpenFlow Controllers manage all the OpenFlow devices and simultaneously each device uses attractor selection in an autonomous manner to achieve his own targets such as reduction of energy consumption, end-to-end delay, and so forth. This combination of a strict control by OpenFlow and a loose control by attractor selection is useful to meet a variety of user needs for the future network.

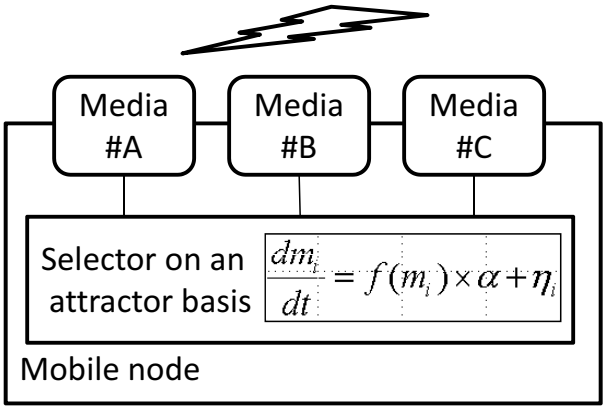

Figure 4.2: An image of multi-interface selection

4.4 Extension of Attractor Selection Model

In this section, we will propose two approaches to enhance the future mobile network infrastructure discussed in Section 4.3 by using the attractor selection method. One is the method of multi-interface selection operating on mobile node side and the other is the method of adaptive clustering method working on network side. Both of them are valid for energy saving to protect environment.

4.4.1 Multi-interface Selection of Mobile Node

In the future mobile network environment, different wireless medium are assumed to be arranged in a mobile node available on cognitive radio infrastructures [61]. The number of access media type, application type, and volume of traffic will increase in a large scale and this kind of explosion in diversity is expected that conventional centralized mobility management and mere distributed mobility management can not work properly and as a matter of fact, existing vertical handovers are not enough to live on the future mobile network. There needs scalable and robust mechanisms and therefore we focus on the attractor selection with the feature of bio-logically inspired mechanism. In the future mobile network, the performance of the best interface for a mobile node might be fluctuating according to environmental changes especially because of the diversity. It should be selected based on

several aspects such as radio quality, traffic distribution, and required QoS. Handling all the conditions by the OpenFlow controller is inefficient and hence a kind of abstract control mechanism should be installed.

We chose the attractor selection model from [59] and the activity equation has been extended to work in a more effective manner by using live traffic information instead of passive pre-defined QoS information. Our proposed model is as follows:

$$\frac{dm_i}{dt} = \frac{s(\alpha)}{1 + max\left(m_i\right)^2 - m_i^2} - d(\alpha)m_i + \eta_i \tag{4.2}$$

$$s(\alpha) = \alpha\left(\beta\alpha^{\gamma} + 1/\sqrt{2}\right),\ d(\alpha) = \alpha \tag{4.3}$$

$$\alpha = \begin{cases} 1/\left(1 + \exp(-G_i m_i)\right) & (m_i > 0) \\ 0 & (m_i = 0) \end{cases} \tag{4.4}$$

where m_i indicates selection fitness of each radio interface of a mobile node and η_i is white Gaussian noise. β and γ are system parameters to design the depth of the potential at the attractor and the strength attracted by activity, respectively. $\alpha\,(0 \leq \alpha \leq 1)$ is activity to express suitability of the selected interface for the current environment, which is expressed as the outputs of sigmoid function of m_i and G_i is a gain parameter. This gain parameter is for the adjustment of sensitivity between activity α and fitness m_i. The selection fitness on each interface, m_i is calculated by using realtime SNR (Signal-to-Noise Ratio) and available bandwidth calculated with the statistics of packet loss, which are shown in Eqn. (4.5) and Eqn. (4.6), respectively. Hence, fluctuating environmental information like packet loss is embedded implicitly on m_i. This m_i indicates the ratio of necessary QoS against live traffic volume on the radio media and closely related to the activity, which is equivalent to the satisfactory degree of media selection. This dynamics provides us with the selection of the best interfaces, which leads to energy conservation by avoiding unnecessary radio resource consumption and unnecessary signaling cost overhead. In addition, once environmental conditions becomes inappropriate, noise effect increases and the other radio interface will be randomly selected in an autonomous manner.

$$\text{realtime SNR} = 2 \times \text{erfc}^{-1}(2 \times \text{BER}) \tag{4.5}$$

$$\text{available bandwidth} = \frac{\text{the volume of successfully received data}}{\text{unit time}} \tag{4.6}$$

where erfc is a complementary error function and this inverse function erfc^{-1} is expressed as follows with the Taylor expansion.

$$\text{BER} = \frac{\text{the volume of successfully received data}}{\text{the volume of transmitted data}}$$

$$\text{erfc}(x) = \frac{2}{\sqrt{(}\pi)} \int_x^\infty \exp^{-t^2}\, dt$$

$$\text{erfc}^{-1}(z) = \sum_{k=0}^{\infty} \frac{c_k}{2k+1} \left(\frac{\sqrt{\pi}}{2} z \right)^{2k+1}$$

In our proposed mechanism, realtime information such as live wireless communication conditions is utilized to drive the above equation and therefore it is expected that additional artificial noise is not necessarily any more if there are sufficient noise on this live traffic information depending on the quality of wireless communications. This is because noise elements are already included in this model. This removal of artificial noise is expected to lead a more light weight management and operating cost reduction thanks to turning off unnecessary functions. In addition, in the case of worse wireless conditions, accurate selection management is not necessary anymore or is even harmful from the viewpoint of system cost. Here, our system based on attractor selection has two modes such as attractor dominant mode and noise dominant mode. Therefore, unnecessary management processes can be avoided in our system and this is one of our benefits, compared with the other systems to count on the accurate decision based on the selection of the interface with the best realtime BER.

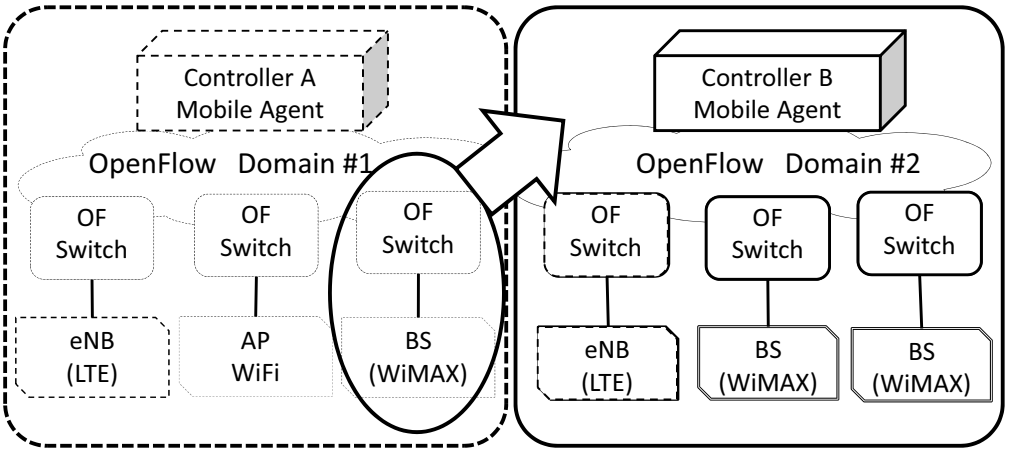

Figure 4.3: An image of dynamic clustering

4.4.2 Adaptive Clustering of Controller Domain

In addition, in the future mobile network, several types of access edge devices are assumed to appear flexibly responding to user needs. Recently, base stations with small coverage like Femto cells [62] are expected to increase in number owing to the growing need for high data rate transmission for richer services. In addition, cognitive radio [61] is another promising technology to accomplish comfortable communication from the viewpoint of efficient frequency usage. Hence, the mixture of different access technologies is most likely to produce more and more opportunities for both vertical and horizontal handovers to cause large amount of signaling traffic between OpenFlow switches and controllers.

We would like to reduce the above signaling cost caused by handovers and utilize attractor selection in adaptively sustaining appropriate clusters according to environmental dynamics from the viewpoint of signaling cost reduction. Here, universality of attractor selection is one of the important features and hence the same basic model is used for this solution. On this issue, the same equations as Eqn. (4.2-4.4) described in previous Subsection 4.4.1 are used, where only m_i is replaced by s_i and s_j indicates selection probability of a cluster group equivalent to each OpenFlow controller relative to a network device such as

routers, base stations, and so forth. Parameters η_j, β, and γ are kept the same as in Section 4.4.1. $\alpha\,(0 \leq \alpha \leq 1)$ is activity to express suitability of the selected cluster equivalent to the OpenFlow controller that the device should join. This activity is expressed as output of a sigmoid function of s_j and K_j is a gain parameter. The selection fitness of each cluster s_j is calculated as the ratio of user data traffic volume against signaling traffic volume by using realtime traffic volume passing through the network device. The larger this value s_j is, the more likely the network device should stay at the current cluster. On the contrary, the smaller it is, the more aggressively the network device should change the cluster that belongs to. Hence, fluctuating environmental information like traffic changes is embedded implicitly on s_j. This s_j indicates the ratio of live traffic volume against signaling traffic volume for the path setup on the cluster media and closely related to the activity, which is equivalent to the satisfactory degree of cluster selection. Therefore, this activity indicates the ratio of user traffic volume against signaling traffic volume for the path setup, which corresponds to high probability to alleviate frequent handovers. This dynamics provides us with the selection of the best clusters, which leads to reduction of frequent users and signaling cost overhead.

According to attractor based dynamics, each network device selects the most appropriate cluster equivalent to OpenFlow controllers. As for attractor selection on OpenFlow controllers themselves, it would work if the OpenFlow network were established in a hierarchical manner. In this scenario, it is assumed that network devices have knowledge about neighboring or reachable OpenFlow controllers in advance. In addition, in the future era, popularity of always-on devices produces less signaling traffic caused by initial power-on procedure than those caused by handovers due to mobility. An example image of clustering is shown in Figure 4.3. The network is divided into clusters A and B surrounded by a dotted line and a straight line, respectively. According to the attractor selection model, some devices of cluster A within the oval are assumed to have a high possibility of handover and therefore are moved to cluster B. This dynamics are expected to formulate the most appropriate cluster distribution from the viewpoint of the optimal signaling cost by handover, in other words, energy cost. However, we should carefully grasp the tradeoff of

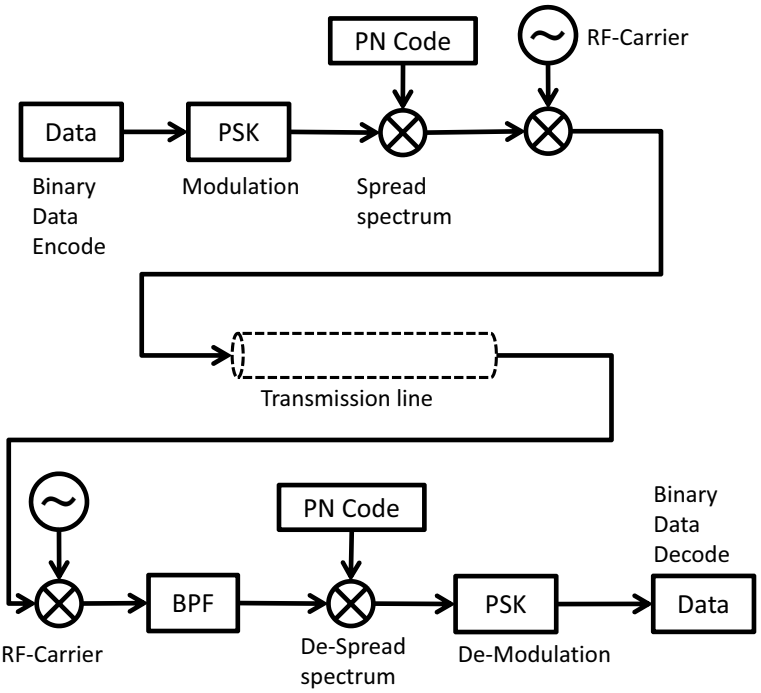

Figure 4.4: A simulation model of transmitter and receiver

reduction of handover cost and increase of cluster switchover cost.

Finally, as stated in the previous section, the effect by utilization of natural noise is also expected on this dynamic clustering solution instead of artificial noise.

4.5 Evaluation of Attractor Selection Extension

In this section, we introduce simulation results of multi-radio interface selection by attractor selection. We simulate wireless communication based on a CDMA (Code Division Multiple Access) channel on a transmission line under a frequency selective fading and analyze basic tendencies of our proposed mechanism.

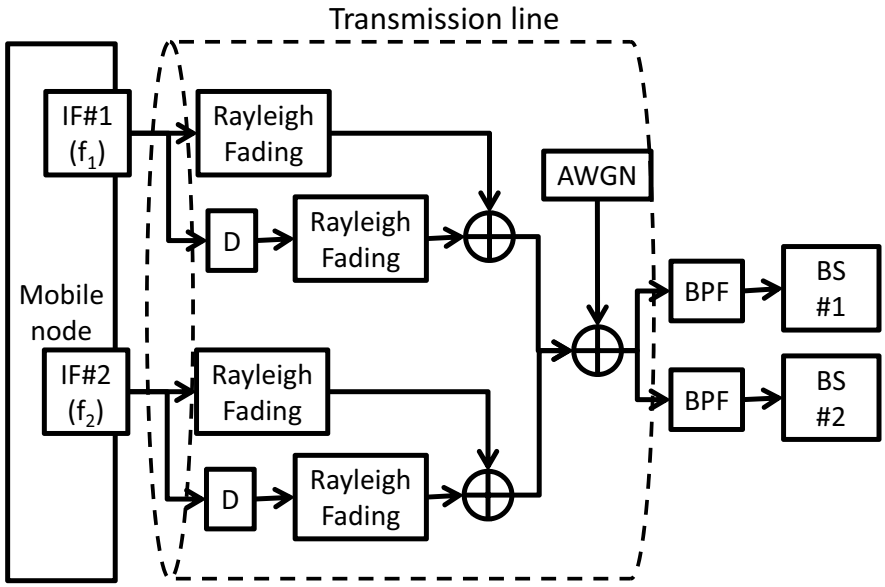

Figure 4.5: A simulation model of transmission line

4.5.1 Simulation Model of Multi-Interface Selection

Basic simulation system model is shown in Figure 4.4. On the transmitter side, binary data is modulated by PSK (Phase Shift Keying), spread by M sequence (maximal length sequence), and transmitted after multiplying carrier frequency. This M sequence is categorized in PN (Pseudo Noise) code due to its code generation approach. On the receiver side, the signal is decoded after being despread and demodulated. As for transmission line, a multi-path fading transmission line is assumed. In Figure 4.5, an example of the transmission line model is described. A mobile node has two radio interfaces with different frequency band usage and each interface is influenced by two path Rayleigh fading [63], whose arrival time difference via each path is expressed as D. In addition, AWGN (Additive White Gaussian Noise) are added after the fading effect to account for shadow fading.

Under the above mentioned conditions, we simulated multi-radio interface selection with our proposed attractor selection mechanism. Basic simulation parameters are listed in Table 4.1. A basic attractor selection function diagram is shown in Figure 4.6. A

Table 4.1: Basic simulation parameters in evaluations of multi-interface selection method

Parameter	**Value**
Number of radio interfaces	2
Spreading code length	31 chip
Chip rate	32 Mcps
Data transmission rate	1 Mbps
Data decision method	Maximum likelihood decision (matched filter)
Carrier frequency	20 MHz
Transmission line model	Additive White Gaussian Noise Two path Rayleigh fading (Delay=1 chip)
Minimum threshold for E_b/N_0	10 dB
Minimum threshold for Bandwidth	100 Hz

selector periodically monitors the statistics of packet transmission on both radio interfaces and calculates realtime based wireless interface SNR (Signal-to-Noise Ratio) and realtime available bandwidth. With them, Yuragi controller select the best radio interface on that condition. Here, Yuragi is a metaphor of noise fluctuation and this fluctuation works for finding the best attractor according to the instantaneous environmental conditions.

In addition, we assume two algorithms for the selector mechanism to choose the best radio interface. The basic selection algorithm and the Yuragi-based selection algorithm are shown in Figures 4.7(a) and 4.7(b), respectively. In Figure 4.7(a), the best interface is first selected at random (Step 1), packet transmission behaviors are monitored (Step 2). Based on the above information, realtime SNR and realtime available bandwidth are calculated (Step 3 and 4). The system has each threshold value of minimum requirement for the SNR and bandwidth. After Step 4, the satisfaction degree of both requirements is checked. If both of them are satisfied, the selector keeps the current radio interface, and on the other hand, if ether of them is not satisfied, it is transfered to Step 1 and starts from the beginning. The best radio interface is maintained by iteration of this cycle. In Figure 4.7(b), the selection process is executed according to Yuragi-based equation and this is expected to generate more smooth shift between radio interfaces. This Yuragi-based attractor selection equation has two features at the same time. One feature is to be

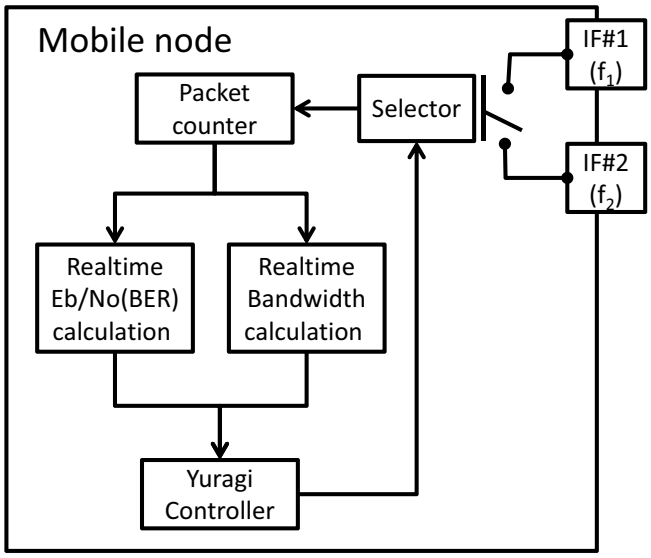

Figure 4.6: Selector function block diagram

converged into an attractor when in good wireless communication condition, which means that it is easy to estimate environmental conditions accurately. The other feature is to select the candidate in a random manner when in bad wireless communication condition, which means that it is hard to predict environmental conditions. Hence, attractor selection has a potential to survive on both good and bad environmental conditions. This is a huge gap between attractor selection and merely greedy selection.

4.5.2 Simulation and Numerical Analysis

Simulation Results of Multi-Interface Selection

Simulation results are shown in this section. The results are obtained on the condition that radio link quality on each interface of mobile node varies as shown in Figure 4.8. This scenario assumes that either interface receives a harmful influence suddenly and for a certain time period. To be exact, radio link quality on interface #0 starts at 40 dB and goes down to 0 dB for the time period from 600 to 1000 time steps and after that it gets back to 40 dB. On the contrary 30 dB is constantly kept on interface #1 during all 1500

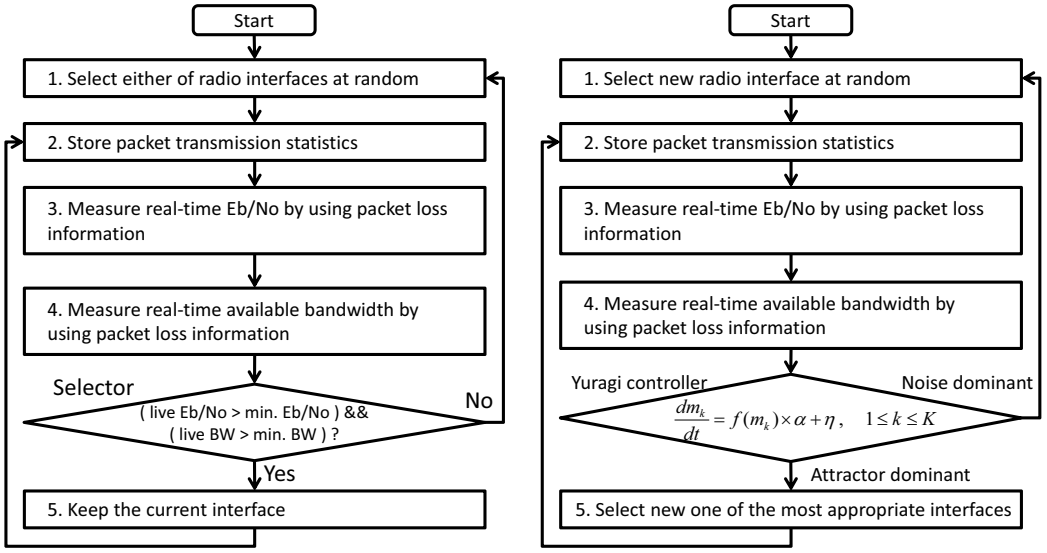

(a) Basic selection algorithm (b) Yuragi-based selection algorithm

Figure 4.7: Examples of selection algorithms

time steps.

The switchover tendencies of the selected active radio interface are shown in Figures 4.9(a), 4.9(b), 4.9(c), and 4.9(d), which are the results in the case that AWGN of the channel is equivalent to 10 dB, 20 dB, 30 dB, and 40 dB, respectively. In Figures 4.9(a) and 4.9(b), it is shown that the best radio interface is fluctuated frequently between interface #0 and #1. This is because in both cases initial noise levels are not so high and therefore the noise level shift by 40 dB as well as the constant noise level difference by 10 dB

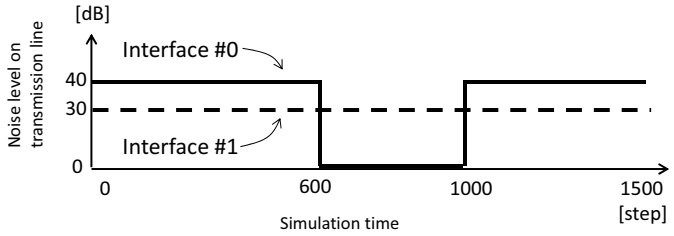

Figure 4.8: Scenario of radio quality changes

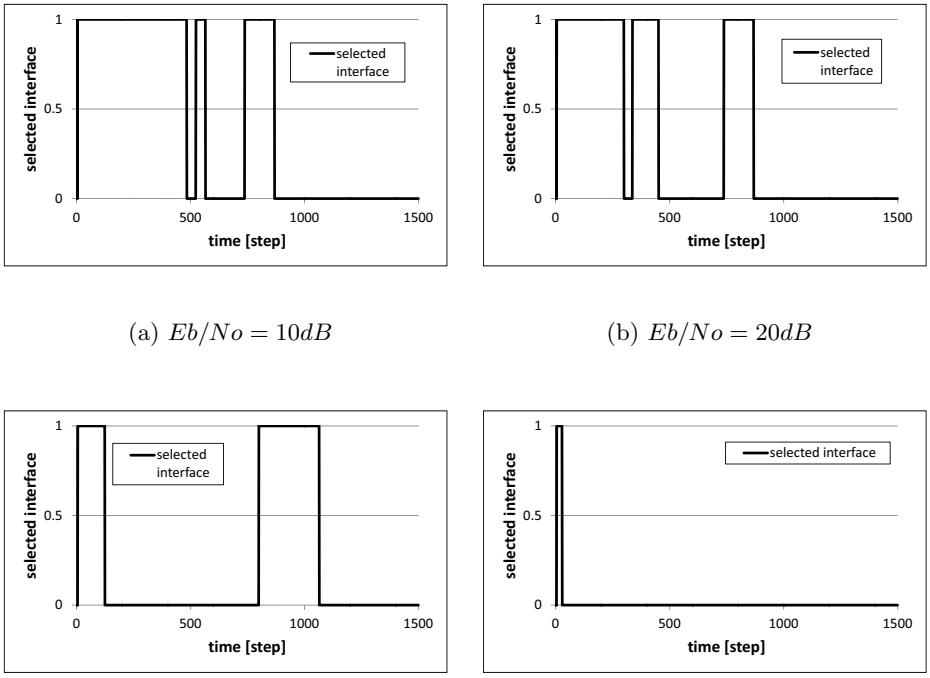

(a) $Eb/No = 10dB$ (b) $Eb/No = 20dB$

(c) $Eb/No = 30dB$ (d) $Eb/No = 40dB$

Figure 4.9: Selected interface change with different level of noises

between interface #0 and #1 doesn't cause any discrepancy in interface selection performance. In this kind of situations, in order to avoid unnecessary interface shifts, a hysteresis mechanism based on forward and backward protection is one of candidates to compensate for it. On the contrary, Figure 4.9(d) shows that initial noise level is so low that any noise level fluctuation doesn't produce any opportunities to shift the best interface and sticks to the radio interface #0 to have an advantage of 10 dB after a transient stage. This is because noise fluctuation is not sufficient to drive the attractor selection mechanism properly. Apart from the above results, in Figure 4.9(c), it is observed that the selected best interface is adjusted according to the noise level shift caused by sudden degradation and recovery from the degradation. From these results, we confirm that our proposed mechanism can not cover all the cases but it is feasible enough for radio interface selection.

In addition, in Figures 4.10(a), 4.10(b), 4.10(c), and 4.10(d), transitions of realtime BER

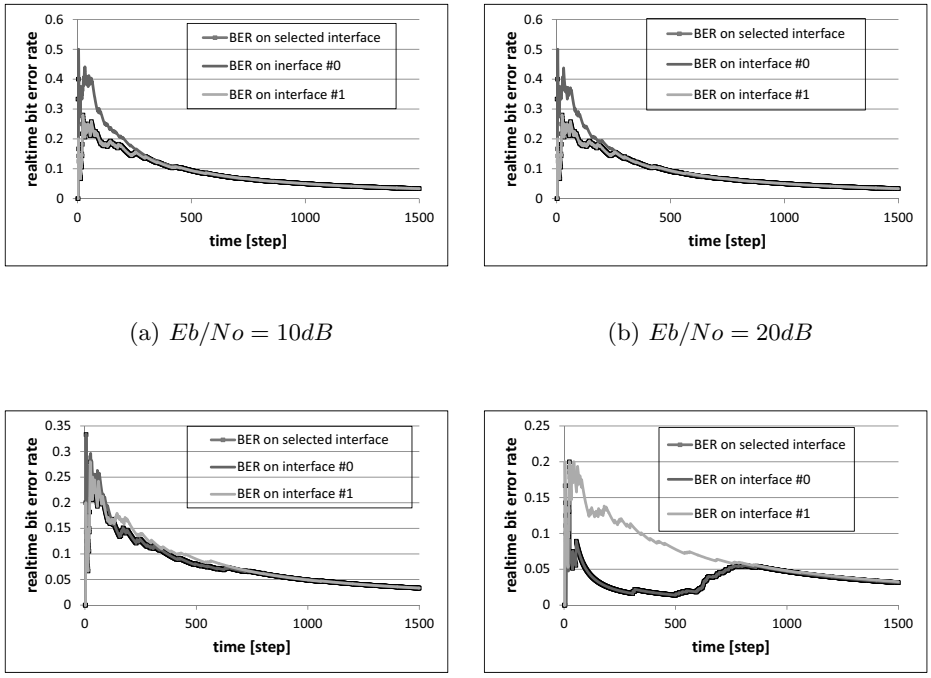

(a) $Eb/No = 10dB$

(b) $Eb/No = 20dB$

(c) $Eb/No = 30dB$

(d) $Eb/No = 40dB$

Figure 4.10: Realtime bit error rate change with different level of noises

(Bit Error Rate) are shown, which are the results in the case that AWGN is equivalent to 10 dB, 20 dB, 30 dB, and 40 dB, respectively. From these results, both cases that the radio interface with better BER is always selected and the initially selected interface does not offer better BER all the time.

Finally, feasibility level against strictness of the threshold parameters is analyzed and shown in Table 4.2. In this table, "strict" means that the threshold is hard to keep its requirements and on the contrary "easy" means that it is possible to keep its requirements in a loose manner. From the result, if either threshold of them are too strict to keep constantly, our proposed attractor selection mechanism is hard to work on. On the other hand, if either of them is easy and the other is not strict, then our proposed attractor selection mechanism work fine. If both are moderate, it depends on the wireless communication conditions. If both are easy, the initial selected attractor will be kept on forever.

Table 4.2: Feasibility against levels of the threshold parameters

Realtime bandwidth	Realtime E_b/N_0		
	Strict	*Moderate*	*Easy*
Strict	Low	Low	Low
Moderate	Low	Normal	High
Easy	Low	High	Very High

Table 4.3: Basic parameters in adaptive clustering cost analysis

Parameter	**Value**
Average packet length	500 bytes (=4000bits)
Average message service rate	0.00025 (=1/4000)
Capacity of channel	2 Mbps
Average session arrival rate	0.001
Number of message hops for one handover	40 hops

Numerical Analysis of Adaptive Cluster Selection

In this section, numerical analysis about adaptive cluster selection is introduced. A network configuration is shown in Figure 4.11. In this figure, two OpenFlow networks are jointly connected in a hierarchical manner. Here, CN, CTL, OFS, and BS indicate Correspondent Node, OpenFlow Controller, OpenFlow Switch, and Base Station, respectively. In addition, small numbers in this figure show the number of hops in message exchanges with reference to the previous cost calculation model for current 3G mobile systems [64]. In addition, basic parameters for cost analysis are shown in Table 4.3. The number of message hops for one inter-domain handover in Table 4.3 is calculated based on a typical inter-domain handover scenario.

The signaling cost incurred by inter-domain handover can be defined as:

$$\text{Cost} = P \times S_{signal} \times H_{signal}$$

where P is the probability that the handover happens, S_{signal} is the average size of signaling sequence, and H_{signal} is the average number of hops for signal traversing. In addition,

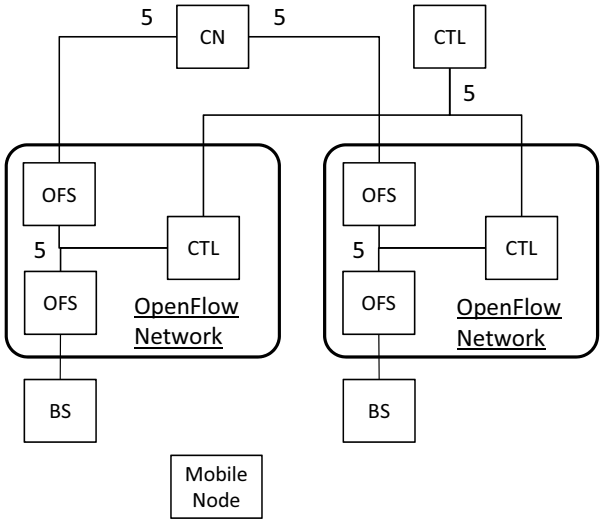

Figure 4.11: Network configuration for clustering cost

making use of concepts of network residence time T_{nr} and session duration time T_{sd}, session arrival probability P_1 and inter-domain handover occurrence probability P_2 are expressed as follows:

$$P_1 = \frac{\lambda\eta}{(\lambda+\eta)^2}$$

$$P_2 = \frac{\eta}{(\mu+\eta)}$$

where λ is the average session arrival rate following a Poisson process, η is the inter-domain mobility ratio that network residence time is exponentially distributed with $1/\eta$, and μ is the average session service rate that session duration time is exponentially distributed with $1/\mu$. Through the above discussion, the cost for inter-domain handover is expressed as follows.

$$\text{Cost} = P_1\lambda\sum_{i}^{n_1}(S_i \times Hi) + P_2\eta\sum_{k}^{n_2}(S_k \times H_k)$$

where n_1 and n_2 are the number of messages for the session arrival and the handover.

Numerical analysis results are shown in Figure 4.12. In this analysis, it is assumed that

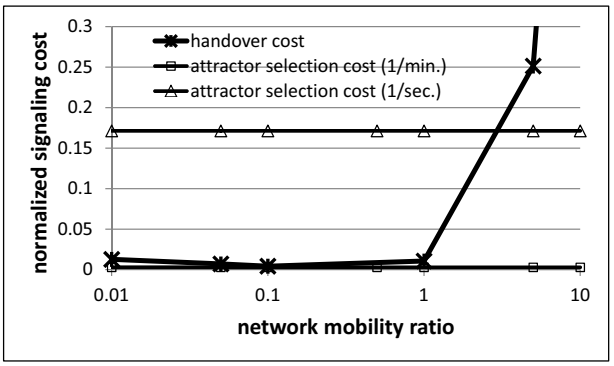

Figure 4.12: Numerical analysis results of handover cost

the OpenFlow controller takes care of 30 OpenFlow switches and the cost caused by inter-domain handover and the cost by repetitive attractor selection are compared. As attractor processing cost, the results with unit processing time of once per second and once per minute are shown. From Figure 4.12, it is observed that in higher network mobility ratio, handover cost is so high that attractor selection is more effective and in lower network mobility ratio, processing once per minute overperforms the handover cost but on the contrary processing once per second is higher than the handover cost. As a result, our proposed method has a potential to produce cost efficiency compared with conventional ordinary inter-domain handover methods.

4.6 Conclusion

In this chapter, we discussed the future mobile network environment and proposed one possibility to combine OpenFlow with attractor selection. In addition, we proposed two novel concepts of mobile network management based on the application of the attractor selection mechanism.

First, we proposed a concept to select the most appropriate interfaces for mobile nodes depending on instantaneous traffic volume. This method uses realtime dynamic information instead of preselected static information as a driving parameter of the attractor selection model, and therefore, the controlling function can be more sensitively operated. In the

end, the network resources are expected to be utilized in an effective way at the right place and at the right moment. Second, a concept to build the most appropriate management domains was proposed. This is targeted to effectively reduce handover signaling cost. In the future, a wide variety of wireless access technologies will bring users more convenience, but bring operators additional management cost at the same time. Hence, we believe that our proposed concepts work and become one of the essential schemes. Finally, simulation results are introduced. Simulation results show that our proposed mechanism is feasible merely by natural noise instead of artificial noise, though depending on the conditions how much noise are received.

Our future work is to evaluate each method based on our concepts by greater variety of simulations to show advantages of our proposal and to formulate specific attractor selection models especially on issues for the future mobile network. In addition, we confirm that they can actually work on a real system through a testbed implementation.

Chapter 5

Conclusion

Mobility functions for communication systems offer flexibility and convenience to users and infrastructures for mobility support require several types of functions. From the architectural viewpoint of a mobility supported system, functions equipped in a centralized manner are easy to install by operators to maintain and offer stereo-typical services. On the other hand, functions equipped in a distributed manner have the potential to provide users with better convenience and higher flexibility. From the viewpoint of protocols in a mobility supported system, mere distributed functions cause an increased complexity of management and hence autonomously self-adaptive mechanisms are necessary to alleviate the complexity to be feasible for communication networks in a large scale. This self-adaptive approach produces a higher robustness for environmentally-fluctuating situations than the centralized one. In addition, in order to make these types of protocols work on practical communication networks, investigation of actual and practical conditions should be taken into account, such as feasibility in heterogeneous wireless networks.

In Chapter 2, we proposed a function-distributed mobility architecture called DisMob for the future Internet. First, we showed qualitative benefits of our proposed method. Then, compared with conventional MIP (Mobile IP) and its extensions, location update cost and packet delivery cost were analyzed for a random walk mobility model from the viewpoint of the mobility method and SMR (Session-to-Mobility Ratio). The cost analysis showed

that DisMob and the MIP extensions have a similar performance and a better performance than MIP. At higher SMR, MIP has more benefits, however at lower SMR, the other three methods are better. In addition, we showed that our proposed function-distributed mobility method showed better performance by cost analysis on a unified localized area in order to cope with overall SMR environment at the same time. Finally, we shared simulation results, confirmed the validity of our numerical analysis, and showed that our proposed function-distributed mobility method is effective and flexible.

In Chapter 3, we proposed a novel mobility assisted firework routing mechanism named Mobility Tolerant Firework Routing to improve packet reachability and we evaluated it by simulations with the the random walk mobility model. In addition, we added a theoretical analysis and proposed an extension to a self-organizing system and evaluated it by simulations. First, we studied the performance of our method from the wireless coverage viewpoint. It turned out that our method showed a good improvement in reachability by the firework effect and the increase in wireless coverage resulted in general in a higher reachability. Next, we analyzed the improvement by firework from the viewpoint of packet reachability, end-to-end delay, and traffic overhead. On all the conditions, it was confirmed that there were large reachability improvements while having slightly additional transmission delay and traffic overhead. The most suitable condition to produce maximum reachability and lowest traffic varied according to the given conditions. Third, we analyzed two parameters, firework threshold and hop limit against packet reachability. We also confirmed that the best values for both parameters exist and they varied depending on system conditions such as wireless transmission environment. In addition, we performed a theoretical analysis from the viewpoint of connectivity for random node distribution. We formulated an equation to express packet reachability and it was confirmed that theoretical results obtained by our formula matched simulation results well. Finally, we proposed an extension of MTFR to a self-organizing system. Simulation results showed that our extended MTFR achieved higher reachability than that generated by simple MTFR. From the above discussion, we confirmed that our method produces improved reachability at the expense of a small additional transmission delay and traffic overhead and we believe that

our proposed method is feasible and achieves higher reachability than standard flooding.

In Chapter 4, we discussed the future mobile network environment and proposed one possibility to work on a large scale to combine OpenFlow with attractor selection. In addition, we proposed two novel concepts of mobile network management based on the extension of the attractor selection mechanism to achieve energy saving from the viewpoint of route calculation and signaling cost. First, we proposed a concept to select the most appropriate interfaces for mobile nodes depending on instantaneous traffic volume. This method uses real-time dynamic information instead of preselected static information as a driving parameter of the attractor selection model, and therefore, the controlling function can be more sensitively operated. In the end, the network resources are expected to be utilized in an effective way at the right place and at the right moment. Second, a concept to build the most appropriate management domains was proposed. This is targeted to effectively reduce handover signaling cost. In the future, a wide variety of wireless access technologies will bring users more convenience, but bring operators additional management cost at the same time. Hence, we believe that our proposed concepts work and become one of the essential schemes. Finally, simulation results are introduced, which show that our proposed mechanism is feasible with adaptability against changes of environmental conditions.

The topics that were studied in this work leave also some room for further improvements. As extension of the mobility-supporting architecture, in Chapter 2, we are planning to include the effects of paging cost and interaction process cost, different mobility models, and more realistic parameter variation, as well as further analytical studies and efficient function placement. Additionally, in Chapter 3, we consider MTFR to have the ability to further improve reachability and can become a better candidate for a safe and secure social communication network infrastructure. Finally, in Chapter 4, our future work is to evaluate the extension of each method based on our concepts by a greater variety of simulations to show advantages of our proposal and to formulate specific attractor selection models especially on issues for the future mobile network. In addition, we intend to confirm that they can actually work on a real system using a testbed implementation.

Bibliography

[1] Telecommunications Carriers Association (TCA), "Number of subscribers by carriers," http://www.tca.or.jp/english/database/2011/10/index.html, Dec. 2011.

[2] Statistics Bureau, Director-General for Policy Planning (Statistical Standards) and Statistical Research and Training Institute, Ministry of Internal Affairs and Communications, Japan, "Statistics bureau home page/result of the population estimates," http://www.stat.go.jp/english/data/jinsui/2.htm, Dec. 2011.

[3] S. Paul, J. Pan, and R. Jain, "Architectures for the future networks and the next generation internet: A survey," *Computer Communications*, vol. 34, pp. 2–42, Jan. 2011. [Online]. Available: http://dx.doi.org/10.1016/j.comcom.2010.08.001

[4] MobilityFirst Future Internet Architecture Project, http://mobilityfirst.winlab.rutgers.edu/.

[5] J. Pan, S. Paul, R. Jain, and M. Bowman, "MILSA: A mobility and multihoming supporting identifier locator split architecture for naming in the next generation internet," in *Proceedings of IEEE Global Communications Conference (GLOBECOM'08)*, Nov. 2008.

[6] OpenFlow Switch Consortium, http://www.openflowswitch.org/.

[7] N. McKeown, T. Anderson, H. Balakrishnan, G. Parulkar, L. Peterson, J. Rexford, S. Shenker, and J. Turner, "OpenFlow: enabling innovation in campus networks,"

ACM SIGCOMM Computer Communication Review, vol. 38, no. 2, pp. 69–74, Apr. 2008.

[8] K.-K. Yap, R. Sherwood, M. Kobayashi, T.-Y. Huangy, M. Chan, N. Handigol, N. McKeown, and G. Parulkar, "Blueprint for introducing innovation into wireless mobile networks," in *Proceedings of the 2nd ACM SIGCOMM International Workshop on Virtualized Infrastructure Systems and Architectures (VISA'10)*, Sep. 2010, pp. 25–32.

[9] K.-K. Yap, M. Kobayashi, R. Sherwood, T.-Y. Huang, M. Chan, N. Handigol, and N. McKeown, "Openroads: empowering research in mobile networks," *ACM SIGCOMM Computer Communication Review*, vol. 40, no. 1, pp. 125–126, Aug. 2010.

[10] C. Perkins, "IP mobility support for IPv4," IETF RFC3344, Aug. 2002.

[11] D. Johnson, C. Perkins, and J. Arkko, "Mobility support in IPv6," IETF RFC3775, Jun. 2004.

[12] R. Koodli, "Mobile IPv6 fast handovers," IETF RFC5568, Jul. 2009.

[13] H. Soliman, C. Castelluccia, K. ElMalki, and L. Bellier, "Hierarchical mobile IPv6 (HMIPv6) mobility management," IETF RFC5380, Oct. 2008.

[14] S. Gundavelli, K. Leung, V. Devarapalli, K. Chowdhury, and B. Patil, "Proxy mobile IPv6," IETF RFC5213, Aug. 2008.

[15] 3GPP TS23.401, "General packet radio service (GPRS) enhancements for evolved universal terrestrial radio access network (E-UTRAN) access," V9.3.0, Dec. 2009.

[16] 3GPP TS23.402, "Architecture enhancements for non-3GPP accesses," V9.3.0, Dec. 2009.

[17] Yuragi Project, http://www.yuragi.osaka-u.ac.jp/index.html.

[18] M. Murata, "Toward establishing ambient network environment," *IEICE Transactions on Communications*, vol. E92-B, no. 4, pp. 1070–1076, Apr. 2009.

[19] G. Motoyoshi, K. Leibnitz, and M. Murata, "Function-distributed mobility system for the future internet," in *Proceedings of 5th IFIP/IEEE International Workshop on Broadband Convergence Networks (BcN'10)*, Osaka, Japan, Apr. 2010.

[20] ——, "Proposal and evaluation of a function-distributed mobility architecture for the future internet," *IEICE Transactions on Communications*, vol. E94-B, no. 7, pp. 1952–1963, Jul. 2011.

[21] ——, "Proposal and evaluation of mobility tolerant firework routing (MTFR)," *Conditionally accepted and re-submitted to IEICE Transactions on Communications, Special Section on Frontiers of Information Network Science*, Nov. 2012.

[22] ——, "MTFR: Mobility tolerant firework routing," in *Proceedings of 4th IEEE International Workshop on Dependable Network Computing and Mobile Systems (DNCMS'11)*, Madrid, Spain, Oct. 2011.

[23] G. Motoyoshi, N. Wakamiya, and M. Murata, "Future mobile network management with attractor selection," in *Proceedings of the 9th IEEE International Conference on Wireless On-demand Network Systems and Services (WONS'12)*. Courmayeur, Italy: IEEE, Jan. 2012.

[24] G. Motoyoshi, K. Leibnitz, and M. Murata, "Proposal and evaluation of a future mobile network management mechanism with attractor selection," *submitted to EURASIP Journal on Wireless Communications and Netowrking, Special Issue on Recent Advances in Optimization Techniques in Wireless Communication Networks*, Jan. 2012.

[25] AKARI Project, "New generation network architecture AKARI conceptual design (ver2.0 in Japanese and ver1.1 in English)," http://akari-project.nict.go.jp/eng/overview.htm.

[26] V. W. S. Wong and V. C. M. Leung, "Location management for next-generation personal communications networks," *IEEE Network Magazine*, vol. 14, no. 5, pp. 18–24, Sep. 2000.

[27] J. S. M. Ho and I. F. Akyildiz, "A dynamic mobility tracking policy for wireless personal communications networks," in *Proceedings of IEEE Global Communications Conference (GLOBECOM'95)*, vol. 1, Nov. 1995.

[28] J. Li, H. Kameda, and K. Li, "Optimal dynamic mobility management for PCS networks," *IEEE/ACM Transactions on Networking*, vol. 8, no. 3, pp. 319–327, Jun. 2000.

[29] K. T. Chen, S. L. Su, and R. F. Chang, "Design and analysis of dynamic mobility tracking in wireless personal communication networks," *IEEE Transactions on Vehicular Technology*, vol. 51, no. 3, pp. 319–327, May 2002.

[30] W. J. Choi and S. Tekinay, "An adaptive location registration scheme with dynamic mobility classification," in *Proceedings of IEEE International Conference on Communications (ICC'02)*, vol. 1, Apr. 2002.

[31] R. Zheng, Y. Ge, J. C. Hou, and S. R. Thuel, "A case for mobility support with temporary home agents," *ACM SIGMOBILE Mobile Computing and Communications Review*, vol. 6, no. 1, pp. 32–46, Jan. 2002.

[32] Y. S. Yen, C. C. Hsu, Y. K. Chan, and H. C. Chao, "Global dynamic home agent discovery on mobile IPv6," in *Proceedings of the 2nd International Conference on Mobile Technology, Applications and Systems*, Nov. 2005.

[33] M. Song, J. Huang, R. Feng, and J. Song, "A distributed dynamic mobility management strategy for mobile IP networks," in *Proceedings of 6th IEEE International Conference on ITS Telecommunications Proceedings*, Jun. 2006, pp. 1045–1048.

[34] P. Bertin, S. Bonjour, and J.-M. Bonnin, "A distributed dynamic mobility management scheme designed for flat IP architectures," in *Proceedings of New Technologies, Mobility and Security (NTMS'08)*, Nov. 2008.

[35] S. Pack and Y. Choi, "A study on performance hierarchical mobile IPv6 in IP-based cellular networks," *IEICE Transactions on Communications*, vol. E87-B, no. 3, pp. 462–469, Mar. 2004.

[36] S. Pack, M. Nam, T. Kwon, and Y. Choi, "A performance comparison of mobility anchor point selection schemes in hierarchical mobile IPv6 networks," *Computer Networks*, vol. 51, no. 6, pp. 1630–1642, Apr. 2007.

[37] B. Singh, "Signaling cost analysis in mobile IP," in *Proceedings of IET International Conference on Wireless, Mobile and Multimedia Networks*, Jan. 2008, pp. 188–191.

[38] A. Basu, A. Lin, and S. Ramanathan, "Routing using potentials: a dynamic traffic-aware routing algorithm," in *Proceedings of ACM SIGCOMM'03*, Aug. 2003, pp. 188–191.

[39] R. Baumann, S. Heimlicher, V. Lenders, and M. May, "HEAT: Scalable routing in wireless mesh networks using temperature fields," in *Proceedings of IEEE Symposium on a World of Wireless, Mobile and Multimedia Networks (WoWMoM'07)*, Jun. 2007.

[40] V. Lenders and R. Baumann, "Link-diversity routing: A robust routing paradigm for mobile ad hoc networks," in *Proceedings of IEEE International Conference Wireless Communications and Networking Conference (WCNC'08)*, vol. 1, Mar. 2008.

[41] D. Y. Kwon, J.-H. Chung, T. Suh, W. G. Lee, and K. Hur, "A potential based routing protocol for mobile ad hoc networks," in *Proceedings of 11th IEEE International Conference on High Performance Computing and Communications (HPCC'09)*, Jun. 2009.

[42] S. Balasubramaniam, J. Mineraud, P. McDonagh, P. Perry, L. Murphy, W. Donnelly, and D. Botvich, "An evaluation of parameterized gradient based routing with QoE monitoring for multiple IPTV providers," *IEEE Transactions on Broadcasting*, vol. 57, no. 2, pp. 183–194, Jul. 2011.

[43] S. Toumpis and L. Tassiulas, "Packetostatics: Deployment of massively dense sensor networks as an electrostatics problem," in *Proceedings of IEEE International Conference on Computer Communications (INFOCOM'05)*, Mar. 2005.

[44] S. Toumpis, "Mother nature knows best: A survey of recent results on wireless networks based on analogies with physics," *Computer Networks*, vol. 52-2, pp. 360–383, Feb. 2008.

[45] C. Bettstetter, "On the minimum node degree and connectivity of a wireless multihop network," in *Proceedings of ACM International Symposium on Mobile Ad Hoc Networking and Computing, 2002 (MobiHoc'02)*, Jun. 2002, pp. 80–91.

[46] M. D. Penrose, "The longest edge of the random minimal spanning tree," *Annals of Applied Probability*, vol. 7, no. 2, pp. 340–361, May 1997.

[47] M. Penrose, "On K-connectivity for a geometric random graph," *Random Structures and Algorithms*, vol. 15, pp. 145–164, Sep. 1999.

[48] P. Gupta and P. R. Kumar, *Critical Power for Asymptotic Connectivity in Wireless Networks*. Birkhauser, May 1999, ch. 4, pp. 547–566.

[49] J. Diaz, D. Mitsche, and X. P.-Gimenez, "Large connectivity for dynamic random geometric graphs," *IEEE Transactions on Mobile Computing*, vol. 8, no. 6, pp. 821–835, Jun. 2009.

[50] T. Hattori, *Random Walk and Renormalization (*in Japanese*)*. Kyoritsu Publishing, Aug. 2004.

[51] K. Leibnitz and M. Murata, "Attractor selection and perturbation for robust networks in fluctuating environments," *IEEE Network, Special Issue on Biologically Inspired Networking*, vol. 24, no. 3, pp. 14–18, May 2010.

[52] S. Balasubramaniam, K. Leibnitz, P. Lio', D. Botvich, and M. Murata, "Biological principles for future internet architecture design," *IEEE Communications Magazine,*

Special Issue on Future Internet Architectures: Design and Deployment Perspectives, vol. 49, no. 7, Jul. 2011.

[53] F. Dressler and O. B. Akan, "Bio-inspired networking: From theory to practice," *IEEE Communications Magazine*, vol. 48, no. 11, Nov. 2010.

[54] M. Meisel, V. Pappas, and L. Zhang, "A taxonomy of biologically inspired research in computer networking," *Computer Networks*, vol. 54, no. 6, pp. 901–916, Apr. 2010.

[55] A. Kashiwagi, I. Urabe, K. Kaneko, and T. Yomo, "Adaptive response of a gene network to environmental changes by fitness-induced attractor selection," *PLoS ONE*, vol. 1, no. 1, p. e49, Dec. 2006.

[56] C. Furusawa and K. Kaneko, "A generic mechanism for adaptive growth rate regulation," *PLoS Computational Biology*, vol. 4, no. 1, p. e3, Jan. 2008.

[57] K. Leibnitz, N. Wakamiya, and M. Murata, "Biologically-inspired self-adaptive multipath routing in overlay networks," *Communications of the ACM, Special Issue on Self-Managed Systems and Services*, vol. 49, no. 3, pp. 62–67, Mar. 2006.

[58] N. Wakamiya, K. Leibnitz, and M. Murata, "A self-organizing architecture for scalable, adaptive, and robust networking," in *Autonomic Network Management Principles: From Concepts to Applications*, N. Agoulmine, Ed. Elsevier, Nov. 2010, pp. 119–140.

[59] S. Kajioka, N. Wakamiya, and M. Murata, "Proposal and evaluation of adaptive resource allocation among multiple nodes and applications in cognitive wireless networks," IEICE, Tech. Rep. NS2009-197, Mar. 2009.

[60] Y. Koizumi, T. Miyamura, S. Arakawa, E. Oki, K. Shiomoto, and M. Murata, "Adaptive virtual network topology control based on attarctor selection," *IEEE Journal of Lightwave Technology*, vol. 28, no. 11, pp. 1720–1731, Jun. 2010.

[61] J. Mitola III and J. G. Q. Maguire, "Cognitive radio: making software radios more personal," *IEEE Personal Communications*, vol. 6, no. 4, Aug. 1999.

[62] V. Chandrasekhar, J. G. Andrews, and A. Gatherer, "Femtocell networks: A survey," *IEEE Communications Magazine*, vol. 46, no. 9, pp. 59–67, Sep. 2009.

[63] W. C. Jakes, *Microwave Mobile Communications*. IEEE Press, May 1994.

[64] K. S. Munasinghe and A. Jamalipour, "Analyiss of signaling cost for a roaming user in a heterogeneous mobile data network," in *Proceedings of IEEE Global Telecommunications Conference (GLOBECOM'08)*, Dec. 2008.

Appendix A

Calculation of Location Update Cost

In this chapter, location update cost formulae for MIP, HMIP, and DynMob are shown. Each parameter has the same meaning as in Section 2.2.2.

A.1 MIP Location Update Cost

Firstly, in the case of MIP, let C_g be the location update cost. This location update procedure is executed all the time globally, irrespective of the mobile node's geographic position. Then, the location update cost is calculated as follows:

$$C_{loc} = \frac{1}{\overline{\overline{T}}} C_g$$

with

$$C_g = 2\left[\kappa + \tau\left(D_v + D_h\right)\right] + N_{CN}\left(2\left[\kappa + \tau\left(D_v + D_c\right)\right] + PC_{CN}\right) + PC_{HA}$$

A.2 HMIP Location Update Cost

Secondly, in the case of HMIP, let C_g and C_l be the global location update cost and localized location update cost, respectively. Global location update is performed when the MN in the boundary ring R moves in an outward direction. In other situations, the MN performs a localized location update. The location update cost is calculated as follows:

$$C_{loc} = \frac{1}{\overline{T}} \left(\pi_R \, \alpha_{R,R+1} C_g + (1 - \pi_R \alpha_{R,R+1}) \, C_l \right)$$

with

$$C_g = 2 \left[\kappa + \tau \left(D_v + D_h \right) \right] + N_{CN} \left(2 \left[\kappa + \tau \left(D_v + D_c \right) \right] + PC_{CN} \right) + PC_{HA} + PC_{MAP}$$
$$C_l = 2 \left(\kappa + \tau D_v \right) + PC_{MAP}$$

A.3 DynMob Location Update Cost

Finally, in the case of DynMob, let C_H, C_{LD}, and C_{LN} be the global location update cost, localized location update cost with delegation, and localized location update cost without delegation, respectively. Performing global location update means that the MN in the boundary ring R moves in an outward direction. In other situations, the MN performs a localized location update. This delegation is performed in a function-bundled manner and in order to calculate the delegation probability, parameter γ is introduced as the probability with which the MN performs the delegation process. Due to the additional complexity of DisMob with larger localized area and function distribution, the delegation probability γ of DynMob must be larger than that of DisMob, i.e., $\gamma < \omega$ to be efficient. From the above conditions, the location update cost is calculated as follows:

$$C_{loc} = \frac{1}{\overline{T}} \left(\pi_R \, \alpha_{R,R+1} C_H + (1 - \pi_R \alpha_{R,R+1}) \left[\gamma \, C_{LD} + (1 - \gamma) \, C_{LN} \right] \right)$$

with

$$
\begin{aligned}
C_H &= 2\left[\kappa + \tau\left(D_v + D_h\right)\right] + N_{CN}\left(2\left[\kappa + \tau\left(D_v + D_c\right)\right] + PC_{CN}\right) \\
&\quad + PC_{HA} + PC_{HA_d} + PC_{HA_d^*} \\
C_{LN} &= 2\left(\kappa + \tau D_v\right) + PC_{HA^*} \\
C_{LD} &= 2\left(\kappa + \tau D_v\right) + PC_{HA^*} + PC_{HA_d^*} + PC_{HA_d^{**}}
\end{aligned}
$$

where PC_{xx} represents the processing costs for binding update procedures at each node, where '*' means that the costs are caused by the delegation process; '*' with and without 'd' means the costs to be delegated by another node and to delegate a bundle of functions to another node, respectively.

Appendix B

Bit Error Rate and Complementary Error Function

In this chapter, we would like to talk about the relationship between bit error rate (BER) and complementary error function. Here, a Binary data transmission modulated in PSK (Phase Shift Keying) is assumed as a typical example and then the received signal $r(t)$ is expressed by using the transmitted signal $s(t)$ and the noise on the transmission line $n(t)$ like WGN (White Gaussian Noise) as follows:

$$r(t) = s(t) + n(t)$$

If the transmitted signal exists from time 0 to time T, the unit energy E_b per 1 bit of the transmitted signal is expressed by using the power spectrum of the signal as follows:

$$E_b = \int_0^T s_0^2(t) = \int_0^T s_1^2(t)$$

where, $s_0(t)$ and $s_1(t)$ indicates the signals to transmit space data and marked data, respectively. In correlation detection by maximum likelihood decision, the decision criteria results in positive and negative decision of each correlation difference between received signal $r(t)$

and each transmitted signal $s(t)$. The decision parameter is expressed as follows.

$$\nu = \int_0^T r(t)\left[s_1(t) - s_0(t)\right] dt$$

In addition, the mean μ and the variance σ^2 of this decision parameter can be estimated by taking into account the mutual correlation between signal $s_0(t)$ and $s_1(t)$. In the end, decision error happens in the case that the decision parameter becomes negative and hence its error probability P_e is expressed as follows:

$$\begin{aligned} P_e &= \frac{1}{\sqrt{2\pi}} \int_0^{-\infty} \exp\left[-\frac{(\nu-\mu)^2}{2\sigma^2}\right] d\nu \\ &= \frac{1}{2}\mathrm{erfc}\left(\frac{\mu}{\sqrt{2}\sigma}\right) \\ &= \frac{1}{2}\mathrm{erfc}\left(\sqrt{\frac{E_b(1-M)}{2N_0}}\right) \end{aligned}$$

with

$$\mathrm{erfc}(x) = \frac{2}{\sqrt{\pi}} \int_x^{\infty} \exp(-t^2) dt$$

where M is the mutual correlation value between signal $s_0(t)$ and $s_1(t)$, and N_0 is the power spectrum density of noise. In the case of BPSK (Binary PSK), space data and marked data have no correlation among each other and idealistic maximum BER can be provided when $M = -1$ as follows.

$$BER = \frac{1}{2}\mathrm{erfc}\sqrt{E_b/N_0}$$

Furthermore, SNR (Signal-to-Noise Ratio) equivalent to E_b/N_0 is expressed as follows:

$$E_b/N_0 = \left(\mathrm{erfc}^{-1}\left(2 \times BER\right)\right)^2$$